

The hadronic light-by-light contribution to the muon $g - 2$ from lattice QCD

TOM BLUM

UConn

NORMAN CHRIST

Columbia

MASASHI HAYAKAWA

Nagoya

TAKU IZUBUCHI

BNL/RBRC

LUCHANG JIN

BNL

CHULWOO JUNG

BNL

CHRISTOPH LEHNER

BNL

6 6 2017

First Workshop of the Muon $g-2$ Theory Initiative

Q Center (near Fermilab)

- **Muon anomalous magnetic moment**
- Lattice QCD and HVP contribution
- HLbL contribution
- Point source photon method
- Simulations
 - Muon leptonic light-by-light
 - 139MeV pion $48^3 \times 96$ lattice
 - 135MeV pion on $64^3 \times 128$ lattice
- Infinite volume QED box
- Conclusions and future plans

Accurate Determination of the μ^+ Magnetic Moment*R. L. GARWIN,[†] D. P. HUTCHINSON, S. PENMAN,[‡] AND G. SHAPIRO[§]*Columbia University, New York, New York*

(Received August 4, 1959)

Using a precession technique, the magnetic moment of the positive mu meson is determined to an accuracy of 0.007%. Muons are brought to rest in a bromoform target situated in a homogeneous magnetic field, oriented at right angles to the initial muon spin direction. The precession of the spin about the field direction, together with the asymmetric decay of the muon, produces a periodic time variation in the probability distribution of electrons emitted in a fixed laboratory direction. The period of this variation is compared with that of a reference oscillator by means of phase measurements of the "beat note" between the two. The magnetic field at which the precession and reference frequencies coincide is measured with reference to a proton nuclear magnetic resonance magnetometer. The ratio of the muon precession frequency to that of the proton in the same magnetic field is thus determined to be 3.1834 ± 0.0002 . Using a re-evaluated lower limit to the muon mass, this is shown to yield a lower limit on the muon g factor of $2(1.00122 \pm 0.00008)$, in agreement with the predictions of quantum electrodynamics.

I. INTRODUCTION

RECENT developments in the theory of weak interactions¹ make it appear that many of the properties of the mu meson can be accounted for on the assumption that it enters into interactions in the same way as the electron but has a much larger mass. The electromagnetic properties of the muon, therefore, acquire increased interest as a further test of the identity of the interactions of the two particles.

Quantum electrodynamics² makes the prediction that the magnetic moment of a spin 1/2 Dirac particle is

of detecting the direction of polarization via their asymmetric decay⁶ made possible the measurement of the muon magnetic moment. In the original experiment it was found necessary, to obtain agreement with the asymmetry curve, to assume a value of the moment close to the Dirac prediction. In this way the value was determined to an accuracy of 1%. The Liverpool group,⁷ using an analog time-to-height converter to record the distribution in time of the emitted electrons, achieved an accuracy of 0.7%. A resonance technique, in which the muons were stopped in a large static magnetic



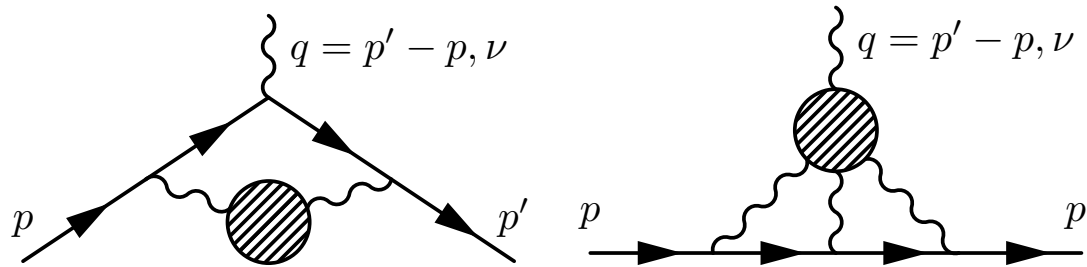
Figure 1. The headstone of Julian Schwinger at Mt Auburn Cemetery in Cambridge, MA.



Figure 2. 1000 Piece Jigsaw Puzzle - Magnetic Moment. \$18.00 from <http://eddata.fnal.gov/>

Almost 4 times more accurate than the previous experiment.

J-PARC E34 also plans to measure muon $g - 2$ with similar precision.



(L) Hadronic vacuum polarization diagram. (R) Hadronic light by light diagram.

	Value \pm Error	Reference
HVP LO ($e^+e^- \rightarrow \text{hadrons}$)	694.9 ± 4.3	Hagiwara et al, 2011
	692.3 ± 4.2	Davier et al, 2011
HVP NLO	-9.84 ± 0.07	Hagiwara et al, 2011
Hadronic Light by Light	10.5 ± 2.6	Glasgow Consensus, 2007
	11.6 ± 4.0	Jegerlehner, Nyffeler, 2009
Standard Model	11659182.8 ± 5.0	
Experiment (0.54 ppm)	11659208.9 ± 6.3	E821, The $g - 2$ Collab. 2006
Difference (Exp - SM)	26.1 ± 8.1	

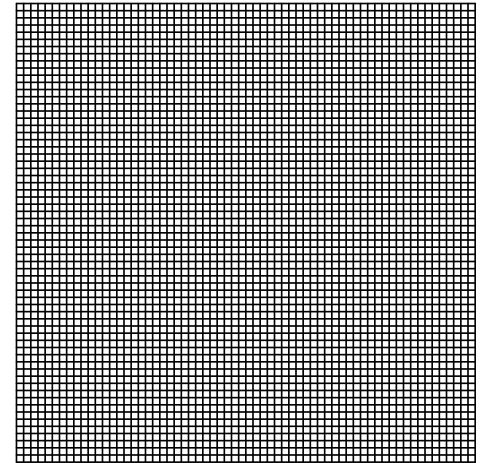
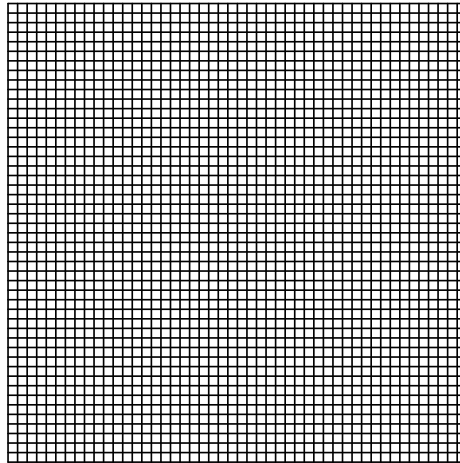
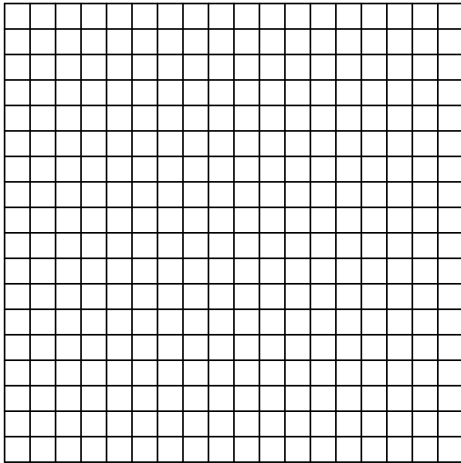
Table 1. Standard model theory and experiment comparison [in units 10^{-10}]

There is 3.3 standard deviations!

- Muon anomalous magnetic moment
- **Lattice QCD and HVP contribution**
- HLbL contribution
- Point source photon method
- Simulations
 - Muon leptonic light-by-light
 - 139MeV pion $48^3 \times 96$ lattice
 - 135MeV pion on $64^3 \times 128$ lattice
- Infinite volume QED box
- Conclusions and future plans

The QCD partition function in Euclidean space time:

$$Z = \int [\mathcal{D}U_\mu] e^{-S_G[U]} \det(D[m_l, U])^2 \det(D[m_s, U]) \quad (1)$$



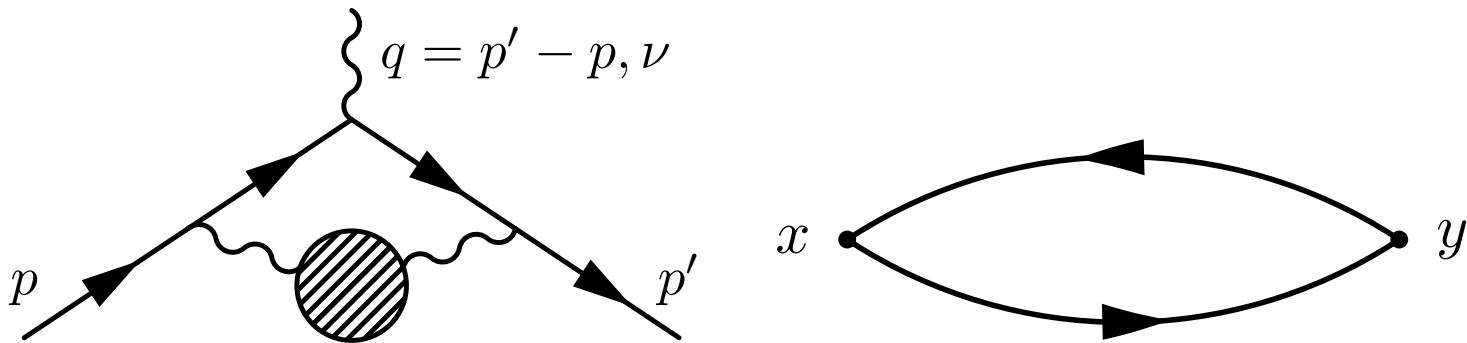
(Left) 19×19 Go board (Middle) 48×48 (Right) 64×64

The configuration is stored in position space. The reason is that the action is local in position space. Working in position makes the calculation simpler.

This is in contrast to analytical perturbative calculation, where interaction only happens occasionally. So it is advantageous to work in momentum space, where the propagator can be diagonalized.

- Many experimental efforts are in the process of obtaining higher precision.
- A lots of lattice of efforts are also trying to compete in this area. Reaching the current experimental accuracy is expected in the next few years. Important cross check!

The major diagram to compute for HVP is:

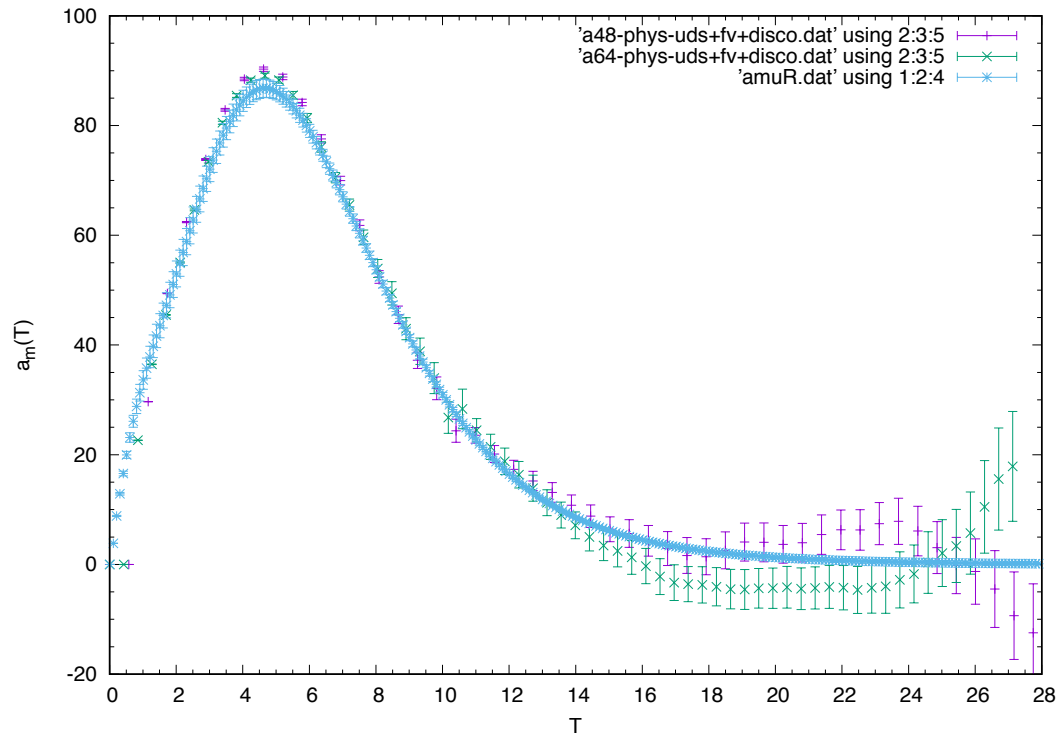


$$F_2(0) = \sum_t w(t) \sum_{\vec{y}} \Pi_{\mu,\nu}(x=0, y=(t, \vec{y})) \quad (2)$$

David Bernecker, Harvey B. Meyer, 2011. arXiv:1107.4388. When $m_\mu t$ is small, we have

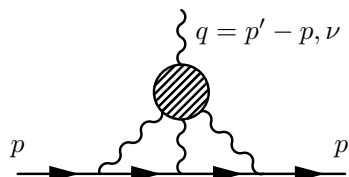
$$w(t) \sim m_\mu^2 t^4 \quad (3)$$

On the lattice, we can use one point source propagator at x to evaluate the diagram.



- The uncertainty of the lattice calculations are mostly in the long distance region.
The uncertainty of the experiments are mostly in the short distance region.
 - Combining the two results may lead to much higher accuracy.
- Tom Blum, Taku Izubuchi, Christoph Lehner, RBC-UKQCD.

- Muon anomalous magnetic moment
- Lattice QCD and HVP contribution
- **HLbL contribution**
- Point source photon method
- Simulations
 - Muon leptonic light-by-light
 - 139MeV pion $48^3 \times 96$ lattice
 - 135MeV pion on $64^3 \times 128$ lattice
- Infinite volume QED box
- Conclusions and future plans



- Frequently used model estimates:

$$a_{\mu}^{\text{HLbL}} = (10.5 \pm 2.6) \times 10^{-10} \quad (\text{Glasgow Consensus. Prades, de Rafael, Vainshtein '09})$$

$$a_{\mu}^{\text{HLbL}} = (11.6 \pm 4.0) \times 10^{-10} \quad (\text{Jegerlehner, Nyffeler '09})$$

- ChPT:

Lowest order for HLbL is pure pion loop (same as scalar QED)

NLO: needs a counterterm (NLO LEC) that is the muon $g - 2$

- Dispersive analysis: (Colangelo et al. '14, '15; Pauk, Vanderhaeghen '14)

Connect contribution to HLbL from presumably numerically dominant light pseudoscalars to in principle measurable form factors and cross-sections.

Need many experimental inputs. Some of them are not available yet.

- "No new physics method" (Experiment - other contributions):

$$[(11659208.9 \pm 6.3) - (11659172.3 \pm 4.3)] \times 10^{-10} = (36.6 \pm 7.6) \times 10^{-10}$$

The HLbL of muon $g - 2$ can also be phrased as:

Sea quark contribution to the magnetic moment of **muon**

An similar quantity is:

Strange sea quark contribution to the magnetic moment of **proton**

- “Determination of the strange nucleon form factors”

Phiala Shanahan, et al. Phys.Rev.Lett. 114 (2015) no.9, 091802.

$G_M^s(Q^2=0) = -0.07 \pm 0.03 \mu_N$ using the “No new physics method”.

- “Strange Quark Magnetic Moment of the Nucleon at the Physical Point”

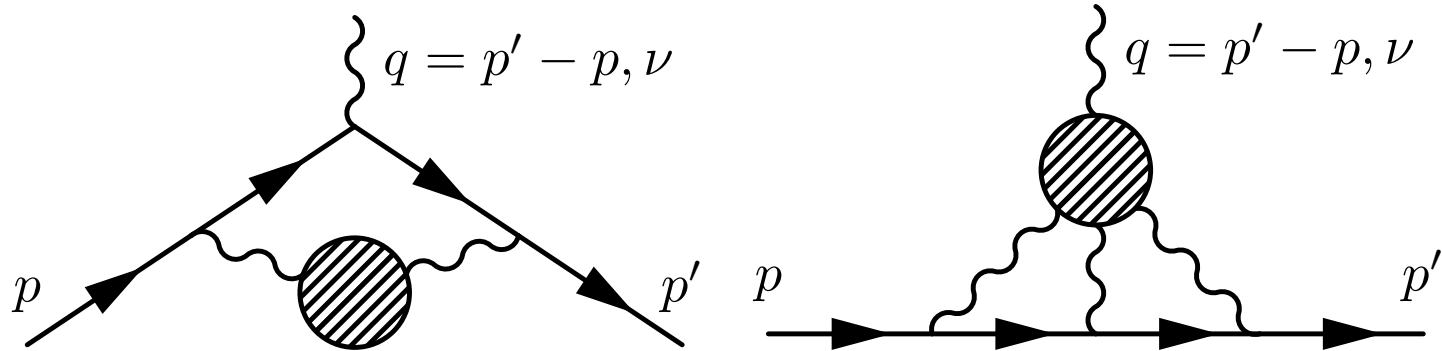
Raza Sabbir Sufian, et al. Phys.Rev.Lett. 118 (2017) no.4, 042001.

$G_M^s(Q^2=0) = -0.064(14)(09) \mu_N$ obtained with direct lattice calculation.

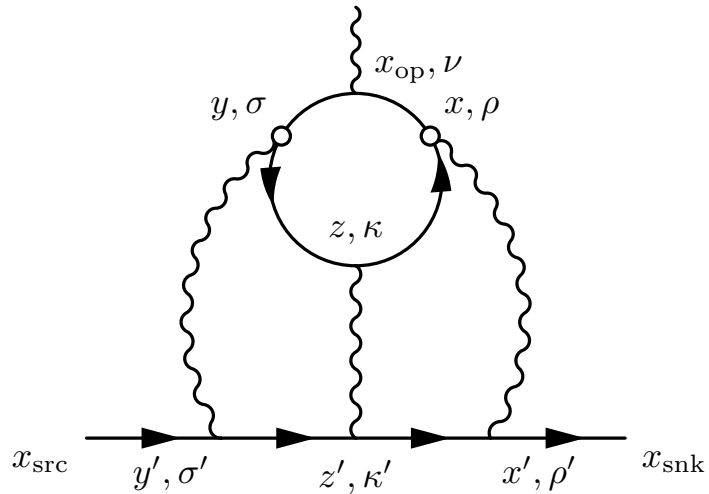
- This subject is started by T. Blum, S. Chowdhury, M. Hayakawa, T. Izubuchi more than 7 years ago. hep-lat/0509016, Phys. Rev. Lett. 114, 012001 (2015).
- A series of improvements in methodology is made later. We computed the connected diagram of HLbL with 171 MeV pion mass. Phys.Rev. D93 (2016) no.1, 014503.
- Mainz group independently come up with a similar method to compute HLbL. Green et al. '15
- With the improved methods, we calculated HLbL using the physical pion mass, $48^3 \times 96$, ensemble. Phys.Rev.Lett. 118 (2017) no.2, 022005.
- Mainz group announces the significant progress on the method to reduce the finite volume effects by treating the QED part of the HLbL diagram semi-analytically in infinite volume. Part of the results are given in Asmussen et al. '16.
- Encouraged by Mainz's success, we use a different approach to compute the QED part of the HLbL in infinite volume. Based the results, we exploit a way to further reduce the lattice discretization error and finite volume error. arXiv:1705.01067.
- Final goal is reaching 10% accuracy to compare with the new experiments.

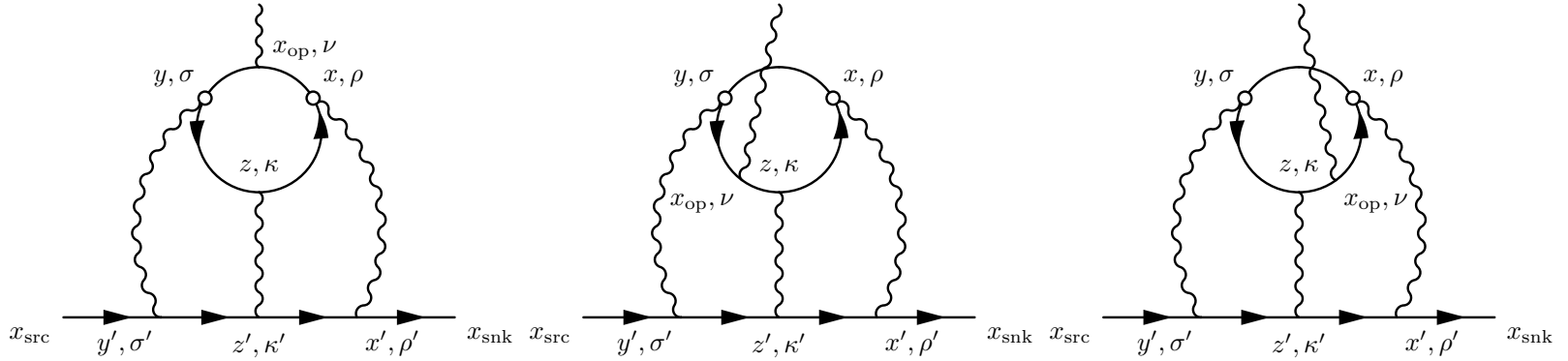
RBC's version of the history on this subject.

- Muon anomalous magnetic moment
- Lattice QCD and HVP contribution
- HLbL contribution
- **Point source photon method**
- Simulations
 - Muon leptonic light-by-light
 - 139MeV pion $48^3 \times 96$ lattice
 - 135MeV pion on $64^3 \times 128$ lattice
- Infinite volume QED box
- Conclusions and future plans



If we can not compute the 4-point function with one point source propagator, use two!





$$\mathcal{F}_\nu^C(\vec{q}; x, y, z, x_{\text{op}}) = (-ie)^6 \mathcal{G}_{\rho, \sigma, \kappa}(\vec{q}; x, y, z) \mathcal{H}_{\rho, \sigma, \kappa, \nu}^C(x, y, z, x_{\text{op}}) \quad (4)$$

$$\begin{aligned} & i^4 \mathcal{H}_{\rho, \sigma, \kappa, \nu}^C(x, y, z, x_{\text{op}}) \\ &= \sum_{q=u, d, s} \frac{(e_q/e)^4}{6} \left\langle \text{tr} \left[-i\gamma_\rho S_q(x, z) i\gamma_\kappa S_q(z, y) i\gamma_\sigma S_q(y, x_{\text{op}}) i\gamma_\nu S_q(x_{\text{op}}, x) \right] \right\rangle_{\text{QCD}} \\ &+ \text{other 5 permutations} \end{aligned} \quad (5)$$

$$\begin{aligned} & i^3 \mathcal{G}_{\rho, \sigma, \kappa}(\vec{q}; x, y, z) \\ &= e^{\sqrt{m_\mu^2 + \vec{q}^2/4}(t_{\text{snk}} - t_{\text{src}})} \sum_{x', y', z'} G_{\rho, \rho'}(x, x') G_{\sigma, \sigma'}(y, y') G_{\kappa, \kappa'}(z, z') \\ & \times \sum_{\vec{x}_{\text{snk}}, \vec{x}_{\text{src}}} e^{-i\vec{q}/2 \cdot (\vec{x}_{\text{snk}} + \vec{x}_{\text{src}})} S_\mu(x_{\text{snk}}, x') i\gamma_{\rho'} S_\mu(x', z') i\gamma_{\kappa'} S_\mu(z', y') i\gamma_{\sigma'} S_\mu(y', x_{\text{src}}) \\ &+ \text{other 5 permutations} \end{aligned} \quad (6)$$

Classically, magnetic moment is simply

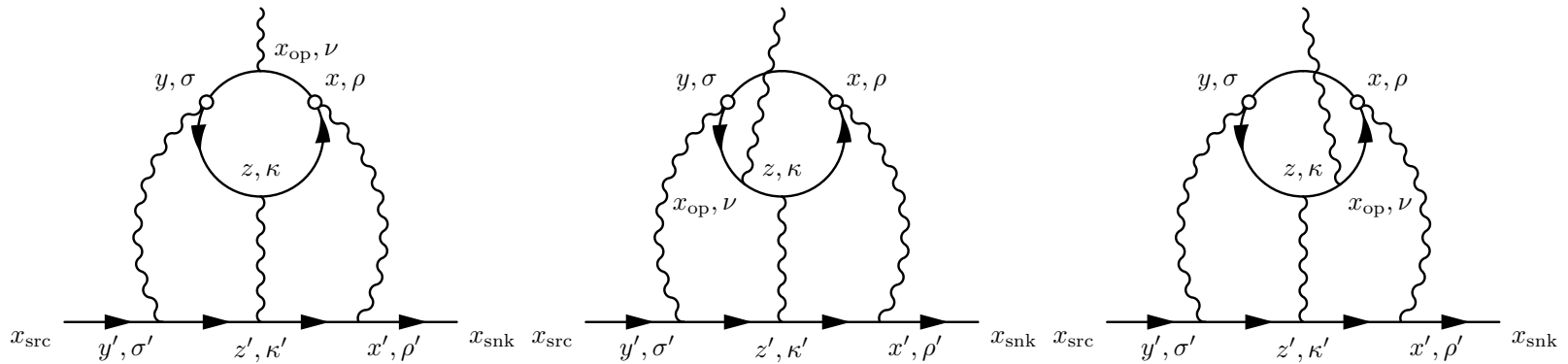
$$\vec{\mu} = \int \frac{1}{2} \vec{x} \times \vec{j} d^3x \quad (7)$$

- This formula is not correct in Quantum Mechanics, because the magnetic moment result from the spin is not included.
- In Quantum Field Theory, Dirac equation automatically predict fermion spin, so the naive equation is correct again!

$$\langle \vec{\mu} \rangle = \left\langle \psi \left| \int \frac{1}{2} \vec{x}_{\text{op}} \times i \vec{j}(\vec{x}_{\text{op}}) d^3x_{\text{op}} \right| \psi \right\rangle \quad (8)$$

- $i \vec{j}(\vec{x}_{\text{op}})$ is the conventional Minkowski spatial current, because of our γ matrix convention.
- The right hand generate the total magnetic moment for the entire system, including magnetic moment from spin.
- Above formula applies to **normalizable state** with zero total current. Not practical on lattice because it need extremely large volume to evaluate.

$$L \gg \Delta x_{\text{op}} \sim 1 / \Delta p \quad (9)$$



$$\frac{F_2(0)}{m} \bar{u}_{s'}(\vec{0}) \frac{\vec{\Sigma}}{2} u_s(\vec{0}) = \sum_r \left[\sum_{z, x_{\text{op}}} \frac{1}{2} \vec{x}_{\text{op}} \times \bar{u}_{s'}(\vec{0}) i\vec{\mathcal{F}}^C\left(\vec{0}; x = -\frac{r}{2}, y = +\frac{r}{2}, z, x_{\text{op}}\right) u_s(\vec{0}) \right]$$

- The initial and final muon states are plane waves instead of properly normalized states.
- Recall the definition for \mathcal{F}_μ , we sum all the internal points over the entire space time except we fix $x + y = 0$.
- The time coordinate of the current, $(x_{\text{op}})_0$ is integrated instead of being held fixed.

These features allow us to perform the lattice simulation efficiently in finite volume.

- One diagram (the biggest diagram below) do not vanish even in the $SU(3)$ limit.
- We extend the method and computed this leading disconnected diagram as well.

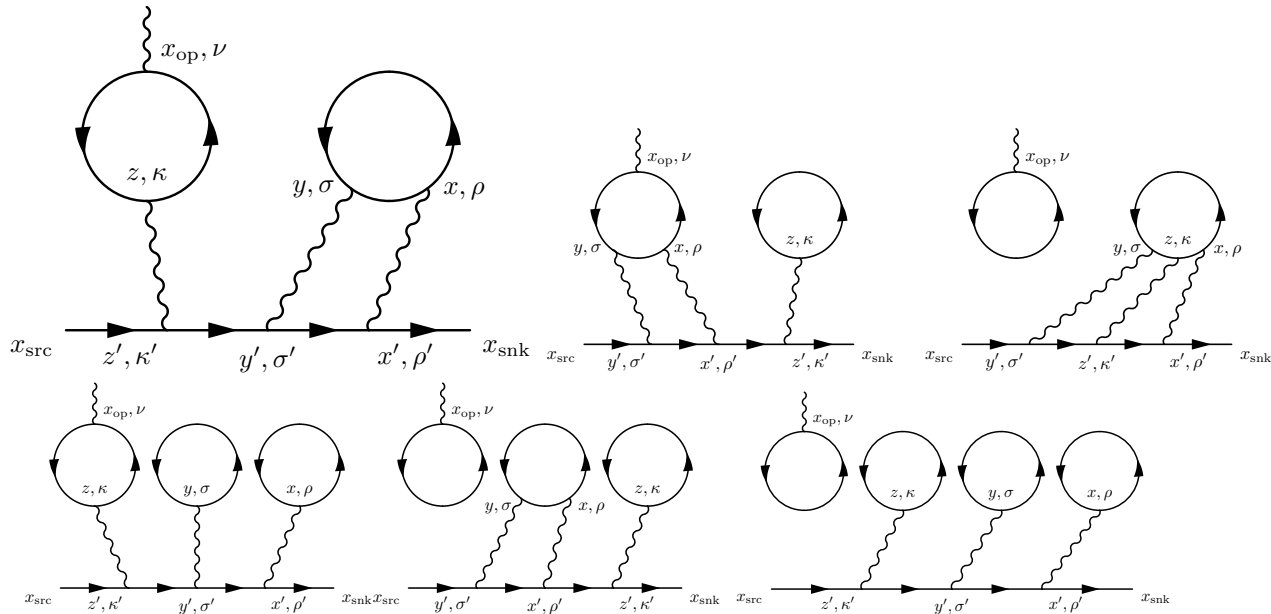
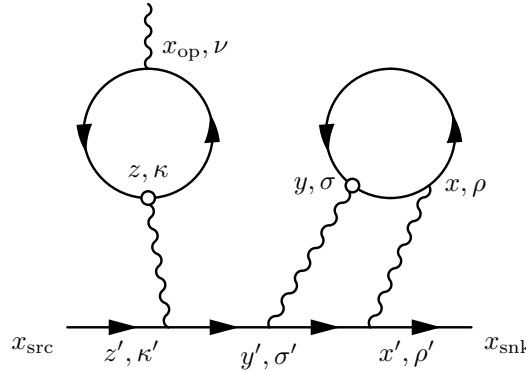


Figure 3. All possible disconnected diagrams. Permutations of the three internal photons are not shown.

- There should be gluons exchange between and within the quark loops, but are not drawn.
- We need to make sure that the loops are connected by gluons by “vacuum” subtraction. So the diagrams are 1-particle irreducible.

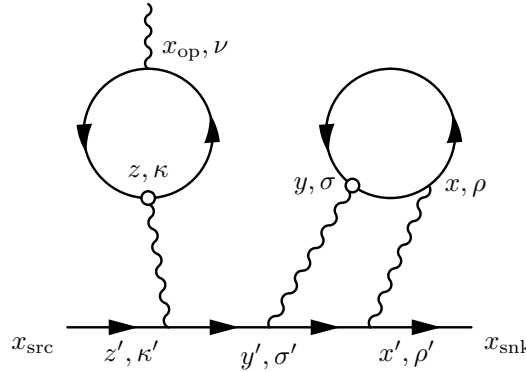


- We can use two point source photons at y and z , which are chosen randomly. The points x_{op} and x are summed over exactly on lattice.
- Only point source quark propagators are needed. We compute M point source propagators and all M^2 combinations of them are used to perform the stochastic sum over $r = z - y$.

$$\mathcal{F}_\nu^D(x, y, z, x_{\text{op}}) = (-ie)^6 \mathcal{G}_{\rho, \sigma, \kappa}(x, y, z) \mathcal{H}_{\rho, \sigma, \kappa, \nu}^D(x, y, z, x_{\text{op}}) \quad (10)$$

$$\mathcal{H}_{\rho, \sigma, \kappa, \nu}^D(x, y, z, x_{\text{op}}) = \left\langle \frac{1}{2} \Pi_{\nu, \kappa}(x_{\text{op}}, z) [\Pi_{\rho, \sigma}(x, y) - \Pi_{\rho, \sigma}^{\text{avg}}(x - y)] \right\rangle_{\text{QCD}} \quad (11)$$

$$\Pi_{\rho, \sigma}(x, y) = - \sum_q (e_q/e)^2 \text{Tr}[\gamma_\rho S_q(x, y) \gamma_\sigma S_q(y, x)]. \quad (12)$$



$$\frac{F_2^{\text{dHLbL}}(0)}{m} \frac{(\sigma_{s',s})_i}{2} = \sum_{r,x} \sum_{x_{\text{op}}} \frac{1}{2} \epsilon_{i,j,k}(\tilde{x}_{\text{op}})_j \cdot i \bar{u}_{s'}(\vec{0}) \mathcal{F}_k^D(x, y=r, z=0, x_{\text{op}}) u_s(\vec{0}) \quad (13)$$

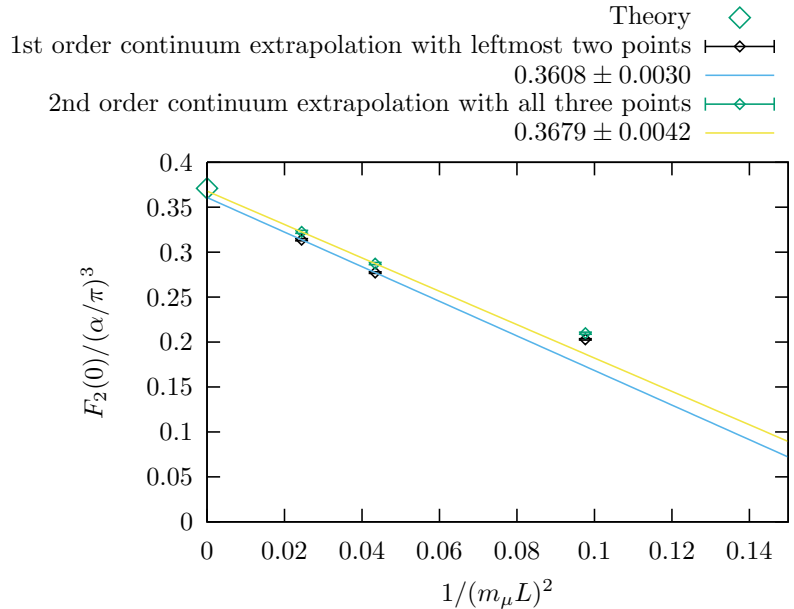
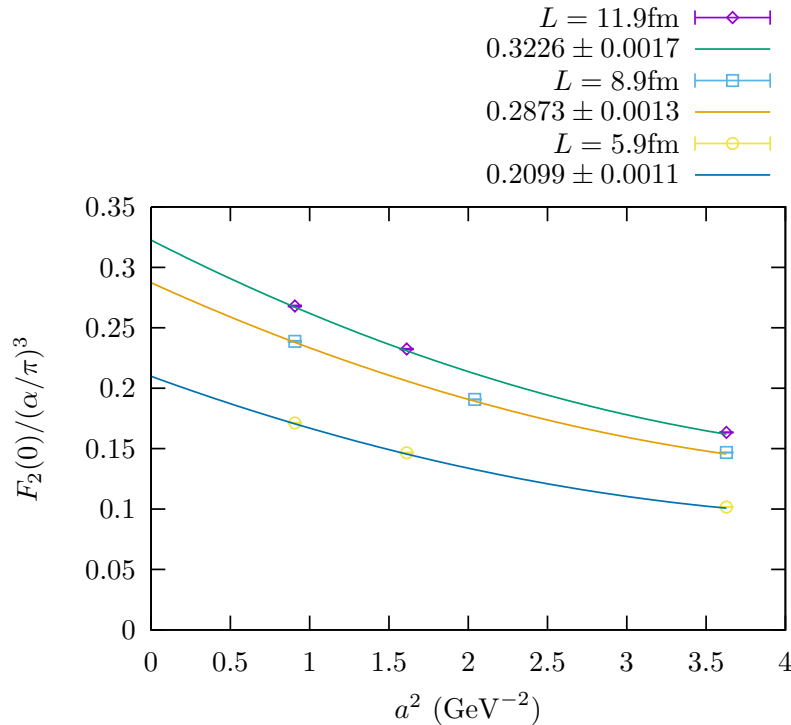
$$\mathcal{H}_{\rho,\sigma,\kappa,\nu}^D(x, y, z, x_{\text{op}}) = \left\langle \frac{1}{2} \Pi_{\nu,\kappa}(x_{\text{op}}, z) [\Pi_{\rho,\sigma}(x, y) - \Pi_{\rho,\sigma}^{\text{avg}}(x - y)] \right\rangle_{\text{QCD}} \quad (14)$$

$$\sum_{x_{\text{op}}} \frac{1}{2} \epsilon_{i,j,k}(x_{\text{op}})_j \langle \Pi_{\rho,\sigma}(x_{\text{op}}, 0) \rangle_{\text{QCD}} = \sum_{x_{\text{op}}} \frac{1}{2} \epsilon_{i,j,k}(-x_{\text{op}})_j \langle \Pi_{\rho,\sigma}(-x_{\text{op}}, 0) \rangle_{\text{QCD}} = 0$$

- Because of the parity symmetry, the expectation value for the left loop average to zero.
- $[\Pi_{\rho,\sigma}(x, y) - \Pi_{\rho,\sigma}^{\text{avg}}(x - y)]$ is only a noise reduction technique. $\Pi_{\rho,\sigma}^{\text{avg}}(x - y)$ should remain constant through out the entire calculation.

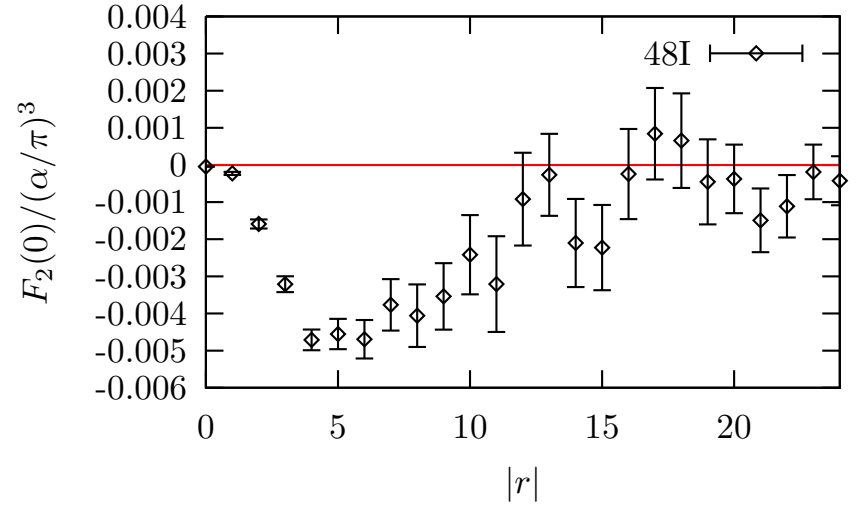
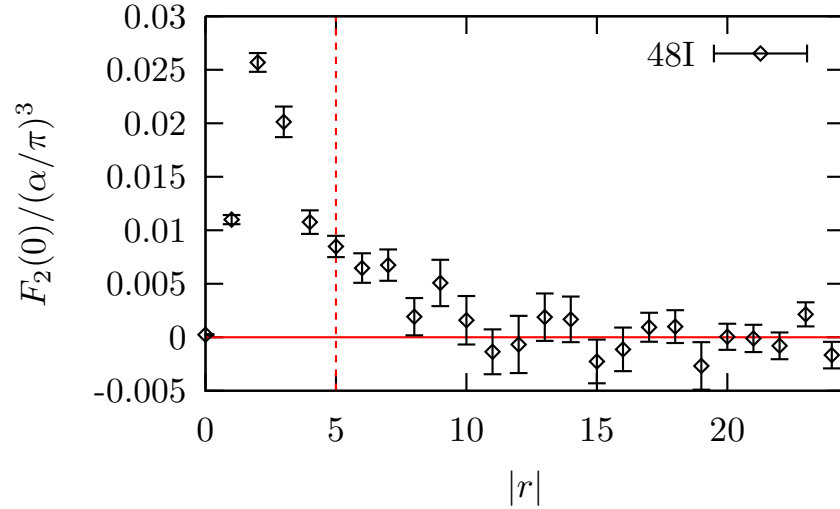
- Muon anomalous magnetic moment
- Lattice QCD and HVP contribution
- HLbL contribution
- Point source photon method
- Simulations
 - **Muon leptonic light-by-light**
 - 139MeV pion $48^3 \times 96$ lattice
 - 135MeV pion on $64^3 \times 128$ lattice
- Infinite volume QED box
- Conclusions and future plans

- We test our setup by computing **muon leptonic light by light** contribution to muon $g - 2$.



- Pure QED computation.** Muon leptonic light by light contribution to muon $g - 2$. Phys.Rev. D93 (2016) 1, 014503. arXiv:1510.07100.
- $\mathcal{O}(1/L^2)$ finite volume effect, because the photons are emitted from a conserved loop.

- Muon anomalous magnetic moment
- Lattice QCD and HVP contribution
- HLbL contribution
- Point source photon method
- Simulations
 - Muon leptonic light-by-light
 - **139MeV pion** $48^3 \times 96$ **lattice**
 - 135MeV pion on $64^3 \times 128$ lattice
- Infinite volume QED box
- Conclusions and future plans



- Left: connected diagrams contribution. Right: leading disconnected diagrams contribution.
- $48^3 \times 96$ lattice, with $a^{-1} = 1.73$ GeV, $m_\pi = 139$ MeV, $m_\mu = 106$ MeV.
- We use Lanczos, AMA, and zMobius techniques to speed up the computations.
- 65 configurations are used. They each are separated by 20 MD time units.

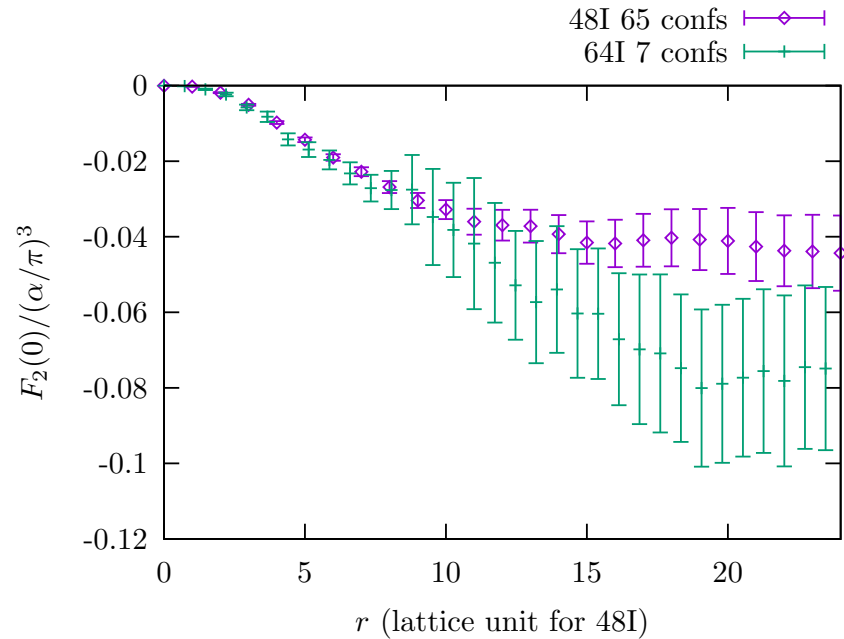
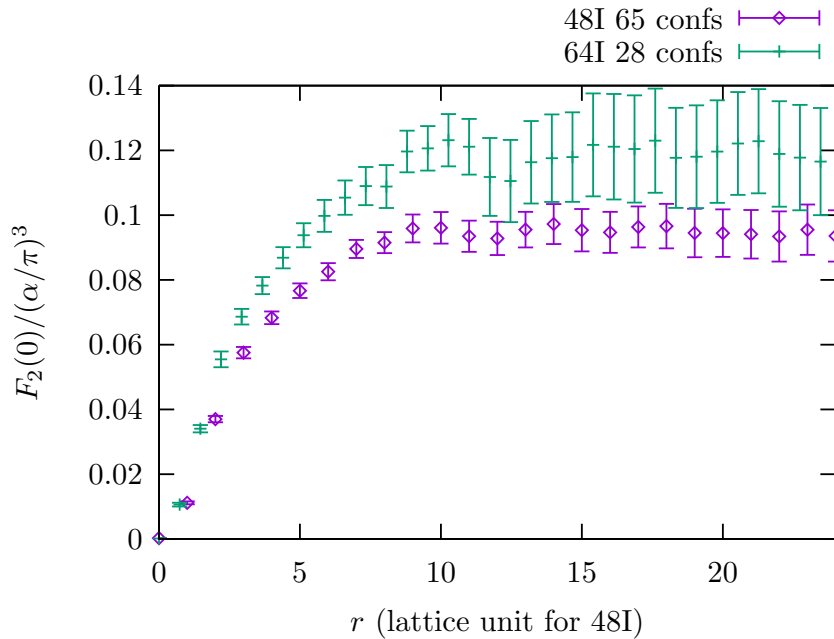
$$\left. \frac{g_\mu - 2}{2} \right|_{\text{cHLbL}} = (0.0926 \pm 0.0077) \times \left(\frac{\alpha}{\pi} \right)^3 = (11.60 \pm 0.96) \times 10^{-10} \quad (15)$$

$$\left. \frac{g_\mu - 2}{2} \right|_{\text{dHLbL}} = (-0.0498 \pm 0.0064) \times \left(\frac{\alpha}{\pi} \right)^3 = (-6.25 \pm 0.80) \times 10^{-10} \quad (16)$$

$$\left. \frac{g_\mu - 2}{2} \right|_{\text{HLbL}} = (0.0427 \pm 0.0108) \times \left(\frac{\alpha}{\pi} \right)^3 = (5.35 \pm 1.35) \times 10^{-10} \quad (17)$$

- Muon anomalous magnetic moment
- Lattice QCD and HVP contribution
- HLbL contribution
- Point source photon method
- Simulations
 - Muon leptonic light-by-light
 - 139MeV pion $48^3 \times 96$ lattice
 - 135MeV **pion on $64^3 \times 128$ lattice**
- Infinite volume QED box
- Conclusions and future plans

This is slightly partial quenched calculation performed on the 139 MeV pion mass ensemble.



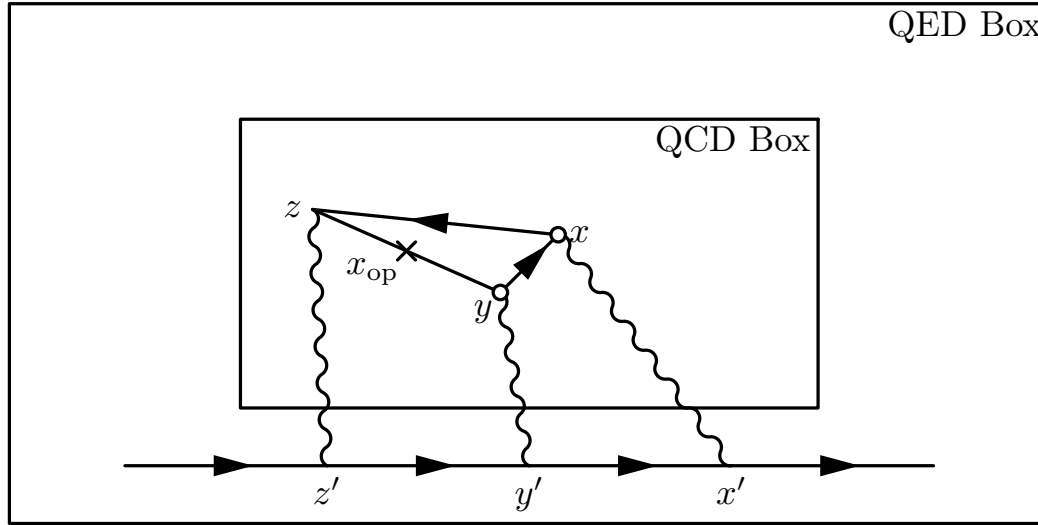
- Left: connected diagrams contribution. Right: leading disconnected diagrams contribution.
- $48^3 \times 96$ lattice, with $a^{-1} = 1.73$ GeV, $m_\pi = 139$ MeV, $m_\mu = 106$ MeV.
- $64^3 \times 128$ lattice, with $a^{-1} = 2.36$ GeV, $m_\pi = 135$ MeV, $m_\mu = 106$ MeV.

- Muon anomalous magnetic moment
- Lattice QCD and HVP contribution
- HLbL contribution
- Point source photon method
- Simulations
 - Muon leptonic light-by-light
 - 139MeV pion $48^3 \times 96$ lattice
 - 135MeV pion on $64^3 \times 128$ lattice
- **Infinite volume QED box**
- Conclusions and future plans

$$\mathcal{F}_\nu^C(x, y, z, x_{\text{op}}) = (-ie)^6 \mathcal{G}_{\rho, \sigma, \kappa}(x, y, z) \mathcal{H}_{\rho, \sigma, \kappa, \nu}^C(x, y, z, x_{\text{op}})$$

The QED part, $\mathcal{G}_{\rho, \sigma, \kappa}(x, y, z)$ can be evaluated in infinite volume QED box.

The QCD part, $\mathcal{H}_{\rho, \sigma, \kappa, \nu}^C(x, y, z, x_{\text{op}})$ can be evaluated in a finite volume QCD box.



$$i^3 \mathcal{G}_{\rho, \sigma, \kappa}(x, y, z) = \mathfrak{G}_{\rho, \sigma, \kappa}(x, y, z) + \mathfrak{G}_{\sigma, \kappa, \rho}(y, z, x) + \text{other 4 permutations.} \quad (18)$$

$$\begin{aligned} \mathfrak{G}_{\rho, \sigma, \kappa}(x, y, z) &= e^{m_\mu(t_{\text{snk}} - t_{\text{src}})} \sum_{x', y', z'} G_{\rho, \rho'}(x, x') G_{\sigma, \sigma'}(y, y') G_{\kappa, \kappa'}(z, z') \\ &\times \sum_{\vec{x}_{\text{snk}}, \vec{x}_{\text{src}}} S_\mu(x_{\text{snk}}, x') i\gamma_{\rho'} S_\mu(x', y') i\gamma_{\sigma'} S_\mu(y', z') i\gamma_{\kappa'} S_\mu(z', x_{\text{src}}) \end{aligned} \quad (19)$$

How to evaluate $\mathfrak{G}_{\rho,\sigma,\kappa}(x, y, z)$? arXiv:1705.01067.

First, we need to regularize the infrard divergence in $\mathfrak{G}_{\rho,\sigma,\kappa}(x, y, z)$.

$$\mathfrak{G}_{\rho,\sigma,\kappa}(x, y, z) = \frac{1 + \gamma_0}{2} [(a_{\rho,\sigma,\kappa}(x, y, z))_k \Sigma_k + i b_{\rho,\sigma,\kappa}(x, y, z)] \frac{1 + \gamma_0}{2} \quad (20)$$

where $a_{\rho,\sigma,\kappa}(x, y, z)$ and $b_{\rho,\sigma,\kappa}(x, y, z)$ are real functions.

$$\mathfrak{G}_{\rho,\sigma,\kappa}^{(1)}(x, y, z) = \frac{1}{2} \mathfrak{G}_{\rho,\sigma,\kappa}(x, y, z) + \frac{1}{2} [\mathfrak{G}_{\kappa,\sigma,\rho}(z, y, x)]^\dagger \quad (21)$$

It turned out that $\mathfrak{G}_{\rho,\sigma,\kappa}^{(1)}(x, y, z)$ is infrard finite.

$$\begin{aligned} \mathfrak{G}_{\rho,\sigma,\kappa}^{(1)}(x, y, z) &= \frac{\gamma_0 + 1}{2} i \gamma_\sigma (\not{\partial}_\zeta + \gamma_0 + 1) i \gamma_\kappa (\not{\partial}_\xi + \gamma_0 + 1) i \gamma_\rho \frac{\gamma_0 + 1}{2} \\ &\times \int \frac{d^4 \eta}{4 \pi^2} \frac{f(\eta - y + \zeta) f(x - \eta + \xi) - f(y - \eta + \zeta) f(\eta - x + \xi)}{2(\eta - z)^2} \Big|_{\xi=\zeta=0} \end{aligned} \quad (22)$$

The 4 dimensional integral is calculated numerically with the CUBA library cubature rules.

Eventually, we need to compute

$$\sum_{x,y,z} \mathfrak{G}_{\rho,\sigma,\kappa}(x, y, z) \mathcal{H}_{\rho,\sigma,\kappa,\nu}^C(x, y, z, x_{\text{op}})$$

$\mathcal{H}_{\rho,\sigma,\kappa,\nu}^C(x, y, z, x_{\text{op}})$ satisfies current conservation condition, which implies:

$$\sum_x \mathcal{H}_{\rho,\sigma,\kappa,\nu}^C(x, y, z, x_{\text{op}}) = 0 \quad (23)$$

$$\sum_z \mathcal{H}_{\rho,\sigma,\kappa,\nu}^C(x, y, z, x_{\text{op}}) = 0 \quad (24)$$

So, we have some freedom in changing $\mathfrak{G}_{\rho,\sigma,\kappa}(x, y, z)$. One choice we find particularly helpful is:

$$\mathfrak{G}_{\rho,\sigma,\kappa}^{(2)}(x, y, z) = \mathfrak{G}_{\rho,\sigma,\kappa}^{(1)}(x, y, z) - \mathfrak{G}_{\rho,\sigma,\kappa}^{(1)}(y, y, z) - \mathfrak{G}_{\rho,\sigma,\kappa}^{(1)}(x, y, y) + \mathfrak{G}_{\rho,\sigma,\kappa}^{(1)}(y, y, y)$$

Consider a vector field $J_\rho(x)$. It satisfies two conditions:

- $\partial_\rho J_\rho(x) = 0$.
- $J_\rho(x) = 0$ if $|x|$ is large.

We can conclude (the result is a little bit unexpected, but actually correct):

$$\int d^4x J_\rho(x) = 0 \quad (25)$$

In three dimension, this result have a consequence which is well-known.

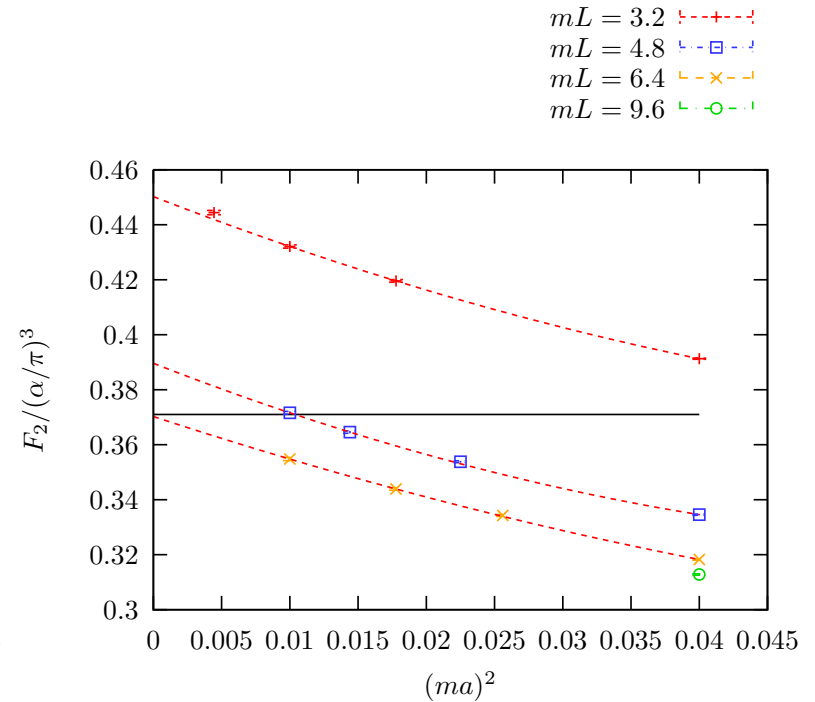
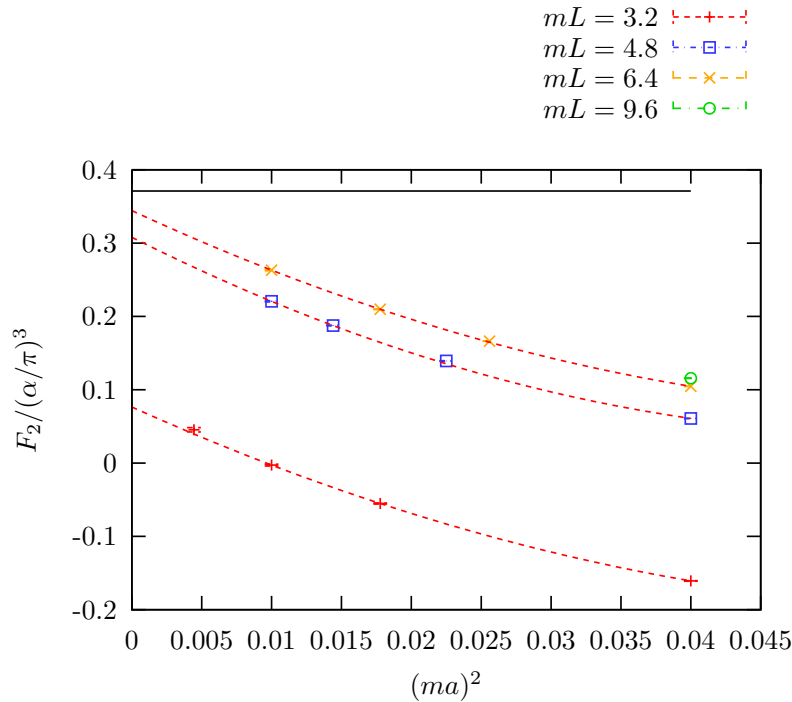
Consider a finite size system with stationary current. We then have

- $\vec{\nabla} \cdot \vec{j}(\vec{x}) = 0$, because of current conservation.
- $\vec{j}(\vec{x}) = 0$ if $|\vec{x}|$ large, because the system is of finite size.

Within a constant external magnetic field \vec{B} , the total magnetic force should be

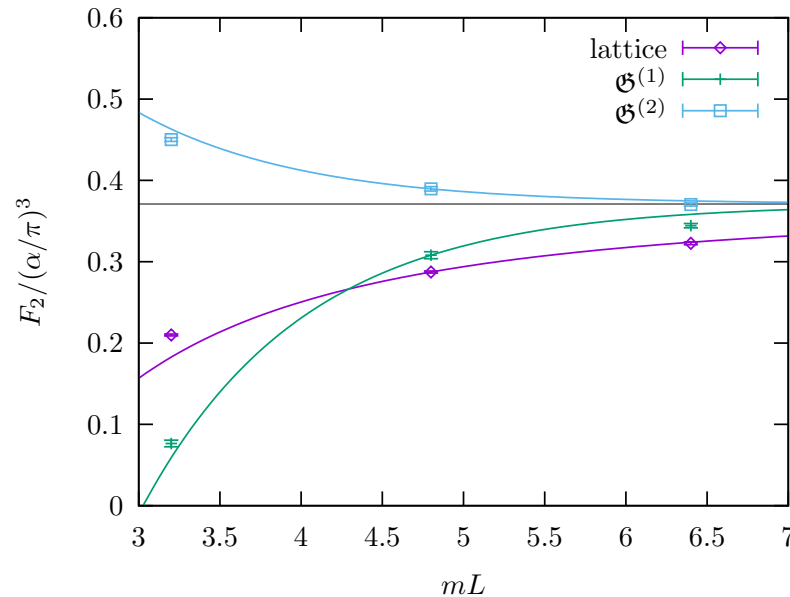
$$\int [\vec{j}(\vec{x}) \times \vec{B}] d^3x = \left[\int \vec{j}(\vec{x}) d^3x \right] \times \vec{B} = 0 \quad (26)$$

- Compare the two $\mathfrak{G}_{\rho,\sigma,\kappa}(x, y, z)$ in **pure QED computation**.



- Left: $\mathfrak{G}^{(1)}$.
- Right: $\mathfrak{G}^{(2)}$. Subtraction is performed on $\mathfrak{G}^{(1)}$.
- Notice the vertical scales in the two plots are different.

- Compare the finite volume effects in different approaches in **pure QED computation**,



- Lattice: $\mathcal{O}(1/L^2)$ finite volume effect, because the photons are emitted from a conserved loop. Phys.Rev. D93 (2016) 1, 014503.
- $\mathcal{G}^{(1)}$: $\mathcal{O}(e^{-mL})$ finite volume effect. Everything except the four-point-correlation function is evaluated in infinite volume. arXiv:1705.01067.
- $\mathcal{G}^{(2)}$: smaller $\mathcal{O}(e^{-mL})$ finite volume effect. arXiv:1705.01067.

- Muon anomalous magnetic moment
- Lattice QCD and HVP contribution
- HLbL contribution
- Point source photon method
- Simulations
 - Muon leptonic light-by-light
 - 139MeV pion $48^3 \times 96$ lattice
 - 135MeV pion on $64^3 \times 128$ lattice
- Infinite volume QED box
- **Conclusions and future plans**

Using the recently developed methods, we have computed the connected hadronic light-by-light contribution with physical pion mass. We use a $48^3 \times 96$ lattice where $L = 5.5\text{fm}$, $m_\pi = 139\text{MeV}$, $m_\mu = 106\text{MeV}$. 65 configurations are used in the calculation.

$$\left. \frac{g_\mu - 2}{2} \right|_{\text{cHLbL}} = (0.0926 \pm 0.0077) \left(\frac{\alpha}{\pi} \right)^3 = (11.60 \pm 0.96) \times 10^{-10} \quad (27)$$

We have extended the methods to cover the leading disconnected diagrams.

$$\left. \frac{g_\mu - 2}{2} \right|_{\text{dHLbL}} = (-0.0498 \pm 0.0064) \left(\frac{\alpha}{\pi} \right)^3 = (-6.25 \pm 0.80) \times 10^{-10} \quad (28)$$

The sum of these two contributions is (significant cancellation between them):

$$\left. \frac{g_\mu - 2}{2} \right|_{\text{HLbL}} = (0.0427 \pm 0.0108) \left(\frac{\alpha}{\pi} \right)^3 = (5.35 \pm 1.35) \times 10^{-10} \quad (29)$$

- We expect rather large finite volume and finite lattice spacing corrections.
- The finite lattice spacing errors can be corrected by performing the same calculation on a finer $64^3 \times 128$ lattice.
- Most of the finite volume errors come from the QED part of the calculations. They can be corrected by perform only the QED part of the calculation in infinite volume with a semi-analytical way.

Thank You!

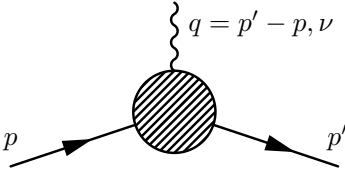
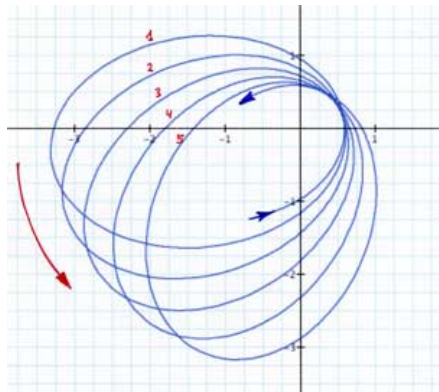
		Value \pm Error	Reference
	Experiment	11659208.9 ± 6.3	E821, $g - 2$ Collab. 2006
	Standard Model ???	11659182.8 ± 5.0 26.1 ± 8.1	Particle Data Group, 2014

Table 2. Standard model theory and experiment comparison [in units 10^{-10}]

Future is hard to predict, let's think of something similar in the history.

Precession of the perihelion of Mercury



	Value \pm Error	Reference
Experiment	574.10 ± 0.65	G. M. Clemence 1947
Newton's Law ???	531.63 ± 0.69 42.47 ± 0.95	G. M. Clemence 1947

Table 3. Newton's Law theory and experiment comparison [in units arcsec/Julian century].

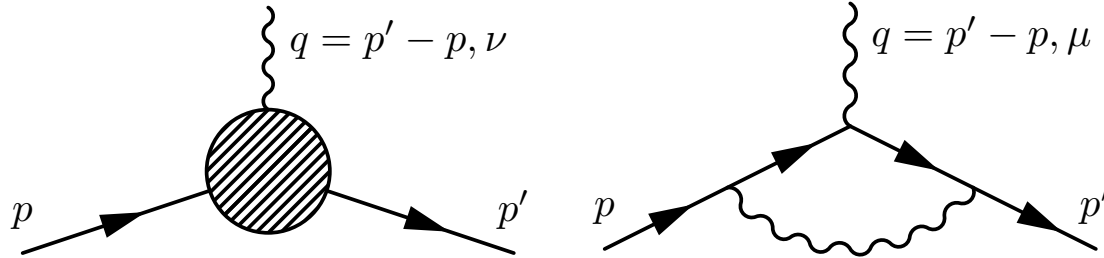


Figure 4. (L) Muon Vertex Function Diagram (R) Schwinger Term Diagram.

$$\begin{aligned}
 \langle \vec{p}', s' | j_\nu(\vec{x}_{\text{op}} = \vec{0}) | \vec{p}, s \rangle &= \left\langle \vec{p}', s' \left| \sum_f q_f \bar{\psi}_f(\vec{x}_{\text{op}} = 0) \gamma_\nu \psi_f(\vec{x}_{\text{op}} = 0) \right| \vec{p}, s \right\rangle \\
 &= -e \bar{u}_{s'}(\vec{p}') \left[F_1(q^2) \gamma_\nu + i \frac{F_2(q^2)}{4m} [\gamma_\nu, \gamma_\rho] q_\rho \right] u_s(\vec{p})
 \end{aligned} \tag{30}$$

$$\vec{\mu} = -g \frac{e}{2m} \vec{s} = -(F_1(0) + F_2(0)) \frac{e}{m} \vec{s} \tag{31}$$

$$F_2(0) = \frac{g-2}{2} \equiv a \tag{32}$$

Use Euclidean convention by default, the relation is

$$\gamma_0 = \gamma_4 = (\gamma^0)^M \quad \gamma = -i\gamma^M \tag{33}$$

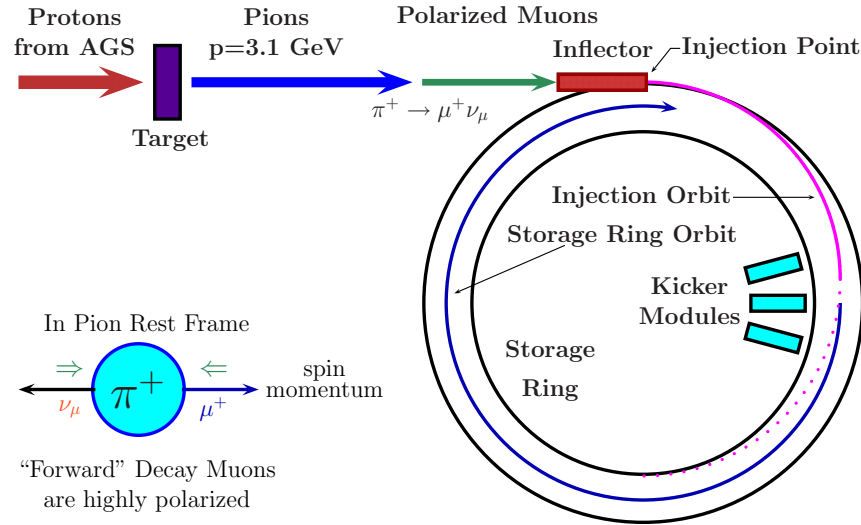


Figure 5. The schematics of muon injection and storage in the $g - 2$ ring. Phys. Rept. **477**, 1 (2009).

$$\omega_c = \frac{e B}{m_\mu \gamma} \quad (34)$$

$$\omega_s = \frac{e B}{m_\mu \gamma} + a_\mu \frac{e B}{m_\mu} \quad (35)$$

$$\gamma = 1/\sqrt{1-v^2} \approx 29.3 \quad (36)$$

Authors	Lab	Muon Anomaly	
Garwin et al. '60	CERN	0.001 13(14)	
Charpak et al. '61	CERN	0.001 145(22)	
Charpak et al. '62	CERN	0.001 162(5)	
Farley et al. '66	CERN	0.001 165(3)	
Bailey et al. '68	CERN	0.001 166 16(31)	
Bailey et al. '79	CERN	0.001 165 923 0(84)	
Brown et al. '00	BNL	0.001 165 919 1(59)	(μ^+)
Brown et al. '01	BNL	0.001 165 920 2(14)(6)	(μ^+)
Bennett et al. '02	BNL	0.001 165 920 4(7)(5)	(μ^+)
Bennett et al. '04	BNL	0.001 165 921 4(8)(3)	(μ^-)

World Average dominated by BNL

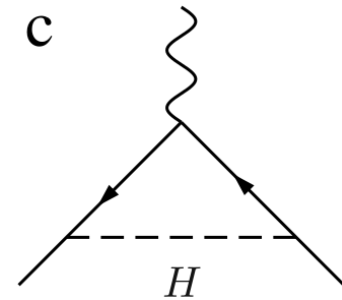
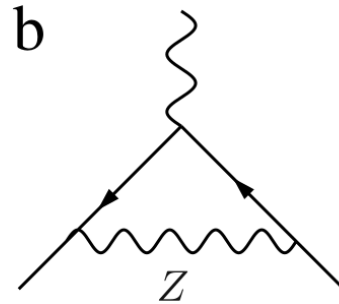
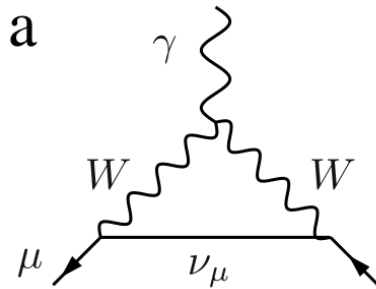
$$a_\mu = (11659208.9 \pm 6.3) \times 10^{-10} \quad (37)$$

In comparison, for electron

$$a_e = (11596521.8073 \pm 0.0028) \times 10^{-10} \quad (38)$$

$$\begin{aligned}
 a_{\mu}^{\text{QED}} &= 0.5 \times \left(\frac{\alpha}{\pi}\right) + 0.765\,857\,425 \underbrace{(17)}_{m_{\mu}/m_{e,\tau}} \times \left(\frac{\alpha}{\pi}\right)^2 \\
 &\quad + 24.050\,509\,96 \underbrace{(32)}_{m_{\mu}/m_{e,\tau}} \times \left(\frac{\alpha}{\pi}\right)^3 + 130.8796 \underbrace{(63)}_{\text{num. int.}} \times \left(\frac{\alpha}{\pi}\right)^4 \\
 &\quad + 753.29 \underbrace{(1.04)}_{\text{num. int.}} \times \left(\frac{\alpha}{\pi}\right)^5 \\
 &= 116\,584\,718.853 \underbrace{(9)}_{m_{\mu}/m_{e,\tau}} \underbrace{(19)}_{c_4} \underbrace{(7)}_{c_5} \underbrace{(29)}_{\alpha(a_e)} [36] \times 10^{-11}
 \end{aligned}$$

Aoyama et al. '12

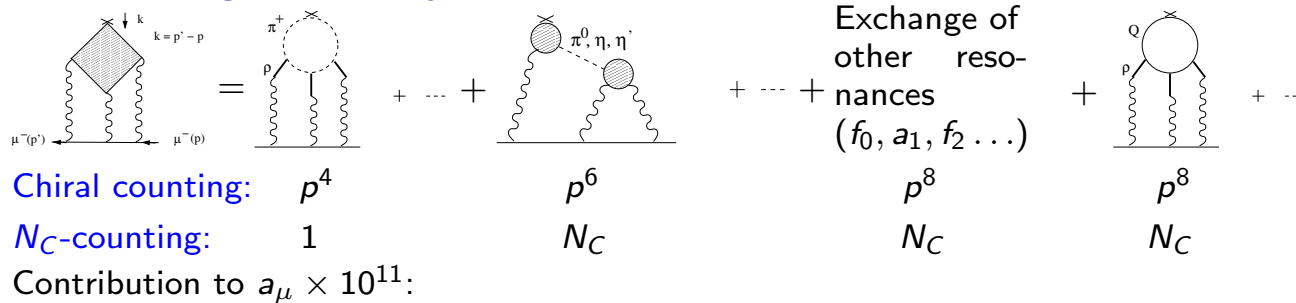


Leading weak contribution. $a = 38.87, b = -19.39, c = 0.00$ [in units 10^{-10}]

	Value \pm Error	Reference
QED incl. 5-loops	11658471.8853 ± 0.0036	Aoyama, et al, 2012
Weak incl. 2-loops	15.36 ± 0.10	Gnendiger et al, 2013

Table 4. Standard model theory, QED and Weak interaction. [in units 10^{-10}]

HLbL scattering: summary of selected results



BPP: +83 (32)	-19 (13)	+85 (13)	-4 (3) [f_0, a_1]	+21 (3)
HKS: +90 (15)	-5 (8)	+83 (6)	+1.7 (1.7) [a_1]	+10 (11)
KN: +80 (40)		+83 (12)		
MV: +136 (25)	0 (10)	+114 (10)	+22 (5) [a_1]	0
2007: +110 (40)				
PdRV: +105 (26)	-19 (19)	+114 (13)	+8 (12) [f_0, a_1]	+2.3 [c-quark]
N,JN: +116 (40)	-19 (13)	+99 (16)	+15 (7) [f_0, a_1]	+21 (3)
ud.: -45		ud.: + ∞		ud.: +60

ud. = undressed, i.e. point vertices without form factors

BPP = Bijmens, Pallante, Prades '96, '02; HKS = Hayakawa, Kinoshita, Sanda '96, '98, '02;
 KN = Knecht, AN '02; MV = Melnikov, Vainshtein '04; 2007 = Bijmens, Prades; Miller, de Rafael,
 Roberts; PdRV = Prades, de Rafael, Vainshtein '09 (compilation; "Glasgow consensus"); N,JN =
 AN '09; Jegerlehner, AN '09 (compilation)

Pseudoscalars: numerically dominant contribution (according to most models !).

Recent reevaluations of axial vector contribution lead to much smaller estimates than in MV '04:
 $a_\mu^{\text{HLbL};\text{axial}} = (8 \pm 3) \times 10^{-11}$ (Pauk, Vanderhaeghen '14; Jegerlehner '14, '15). Would shift
 central values of compilations downwards:

$$a_\mu^{\text{HLbL}} = (98 \pm 26) \times 10^{-11} \text{ (PdRV)} \quad \text{and} \quad a_\mu^{\text{HLbL}} = (102 \pm 40) \times 10^{-11} \text{ (N, JN)}.$$

Recall (in units of 10^{-11}): $\delta a_\mu(\text{HVP}) \approx 45$; $\delta a_\mu(\text{exp [BNL]}) = 63$; $\delta a_\mu(\text{future exp}) = 16$

$$\langle \mathcal{O}[U, \bar{u}, u, \bar{d}, d, \bar{s}, s] \rangle_{\text{QCD}} = \frac{1}{Z} \int [\mathcal{D}U_\mu] e^{-S_G[U]} \int [\mathcal{D}\bar{u}][\mathcal{D}u][\mathcal{D}\bar{d}][\mathcal{D}d][\mathcal{D}\bar{s}][\mathcal{D}s] \cdot e^{\bar{u}D[m_l, U]u + \bar{d}D[m_l, U]d + \bar{s}D[m_s, U]s} \mathcal{O}[U, \bar{u}, u, \bar{d}, d, \bar{s}, s]. \quad (39)$$

A simple example, quark propagator:

$$\begin{aligned} \langle u(x)\bar{u}(y) \rangle_{\text{QCD}} &= \frac{1}{Z} \int [\mathcal{D}U_\mu] e^{-S_G[U]} \det(D[m_l, U])^2 \det(D[m_s, U]) D^{-1}[m_l, U](x, y) \\ &= \langle S_l(x, y) \rangle_{\text{QCD}} \end{aligned} \quad (40)$$

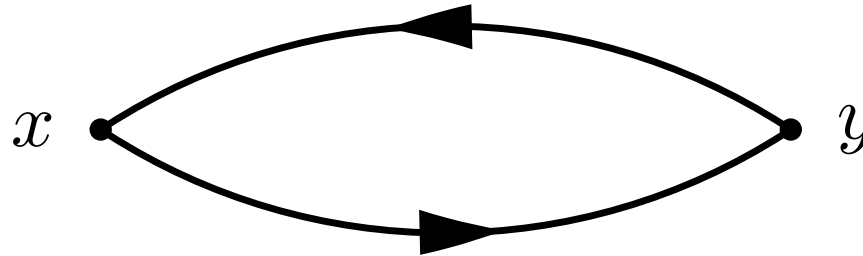
A more realistic example, pion correlation function:

$$\begin{aligned} -\langle \bar{d}(x)\gamma_5 u(x)\bar{u}(y)\gamma_5 d(y) \rangle_{\text{QCD}} &= \frac{1}{Z} \int [\mathcal{D}U_\mu] e^{-S_G[U]} \det(D[m_l, U])^2 \det(D[m_s, U]) \\ &\quad \times \text{Tr}[D^{-1}[m_l, U](x, y)\gamma_5 D^{-1}[m_l, U](y, x)\gamma_5] \\ &= \langle \text{Tr}[S_l(x, y)\gamma_5 S_l(y, x)\gamma_5] \rangle_{\text{QCD}} \\ &= \langle \text{Tr}[S_l(x, y)[S_l(x, y)]^\dagger] \rangle_{\text{QCD}} \end{aligned} \quad (41)$$

$$\sim \frac{1}{|y-x|^{3/2}} e^{-m_\pi|y-x|} \quad (42)$$

$$\langle O(t_2)O(t_1) \rangle_{\text{QCD}} = \langle 0|O(t_2) \exp(-H(t_2 - t_1)) O(t_1)|0 \rangle$$

Charged pion correlation function



$$-\langle \bar{d}(x) \gamma_5 u(x) \bar{u}(y) \gamma_5 d(y) \rangle_{\text{QCD}} = \langle \text{Tr}[S_l(x, y) [S_l(x, y)]^\dagger] \rangle_{\text{QCD}} \quad (43)$$

$$\sim \frac{e^{-m_\pi |y-x|}}{|y-x|^{3/2}} \sim e^{-m_\pi |y-x|} \quad (44)$$

The quantity being averaged is positive semi-definite, thus the statistical error is on the same order as the signal. This implies:

- One can evaluate the charged pion correlation function at very long distance without suffering from the signal to noise problem.
- The typical size of the light quark propagator at long distance is roughly $e^{-\frac{m_\pi}{2}|y-x|}$, this can be used to help us to estimate the size of the noise for many observable.

$$\begin{aligned}
 & \langle \bar{u}(x_{\text{op}}) \gamma_\nu u(x_{\text{op}}) \bar{u}(x) \gamma_\rho u(x) \bar{u}(y) \gamma_\sigma u(y) \bar{u}(z) \gamma_\kappa u(z) \rangle_{\text{QCD}} \\
 &= \langle -\text{tr}[\gamma_\nu S_u(x_{\text{op}}, x) \gamma_\rho S_u(x, z) \gamma_\kappa S_u(z, y) \gamma_\sigma S_u(y, x_{\text{op}})] \rangle_{\text{QCD}} \\
 &+ \langle -\text{tr}[\gamma_\nu S_u(x_{\text{op}}, z) \gamma_\kappa S_u(z, x) \gamma_\rho S_u(x, y) \gamma_\sigma S_u(y, x_{\text{op}})] \rangle_{\text{QCD}} \\
 &+ \text{other 4 permutations} \\
 &+ \text{disconnected contractions}
 \end{aligned} \tag{45}$$

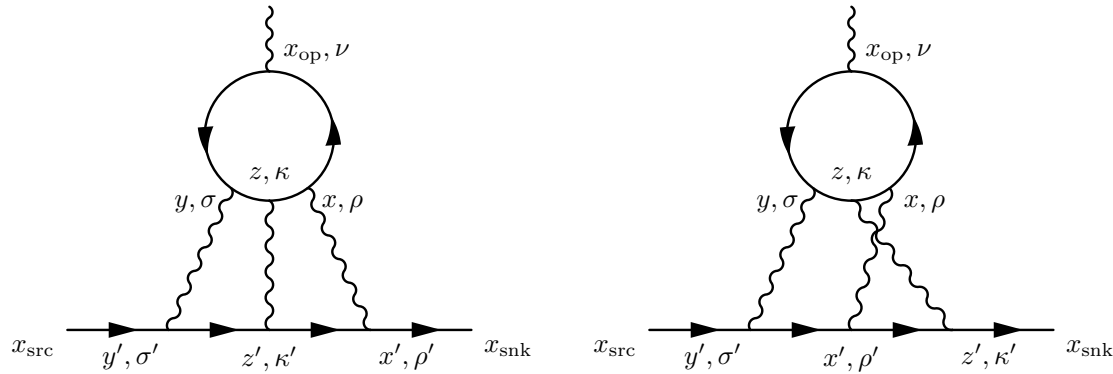


Figure 6. Light by Light diagrams. There are 4 other possible permutations.

- Evaluate the quark and muon propagators in the background quenched QED fields. Thus generate all kinds of diagrams.

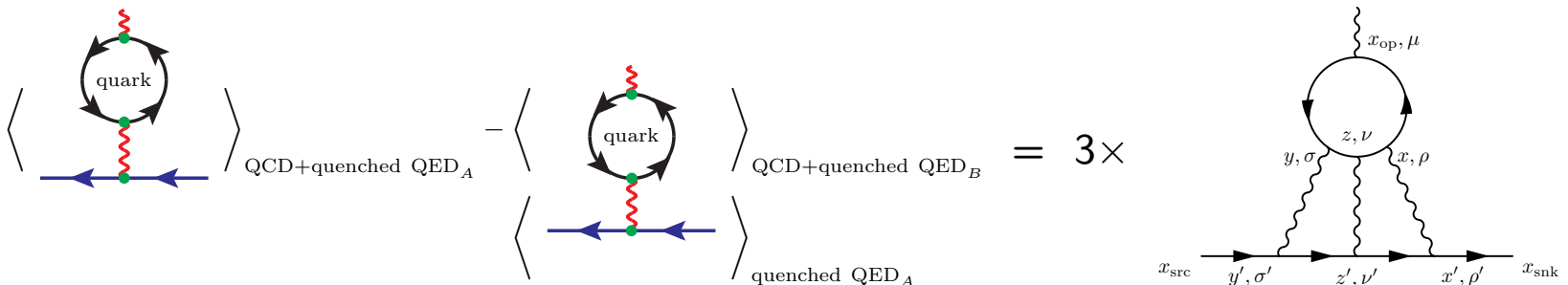


Figure 7. PoS LAT2005 (2006) 353. hep-lat/0509016. One typical diagram remains after subtraction is shown on the left, 5 others are not shown.

- After subtraction, the lowest order signal remains is $\mathcal{O}(e^6)$ which is exact LbL diagram.
- Solved the 3-loop problem. Now we only need to compute point source propagators in the background of QED fields.
- Unwanted higher order effects. In practice, one normally choose $e = 1$.
- Lower order noise problem. The signal after subtraction is $\mathcal{O}(e^6)$. But even after charge conjugation average on the muon line, the noise is still $\mathcal{O}(e^4)$.

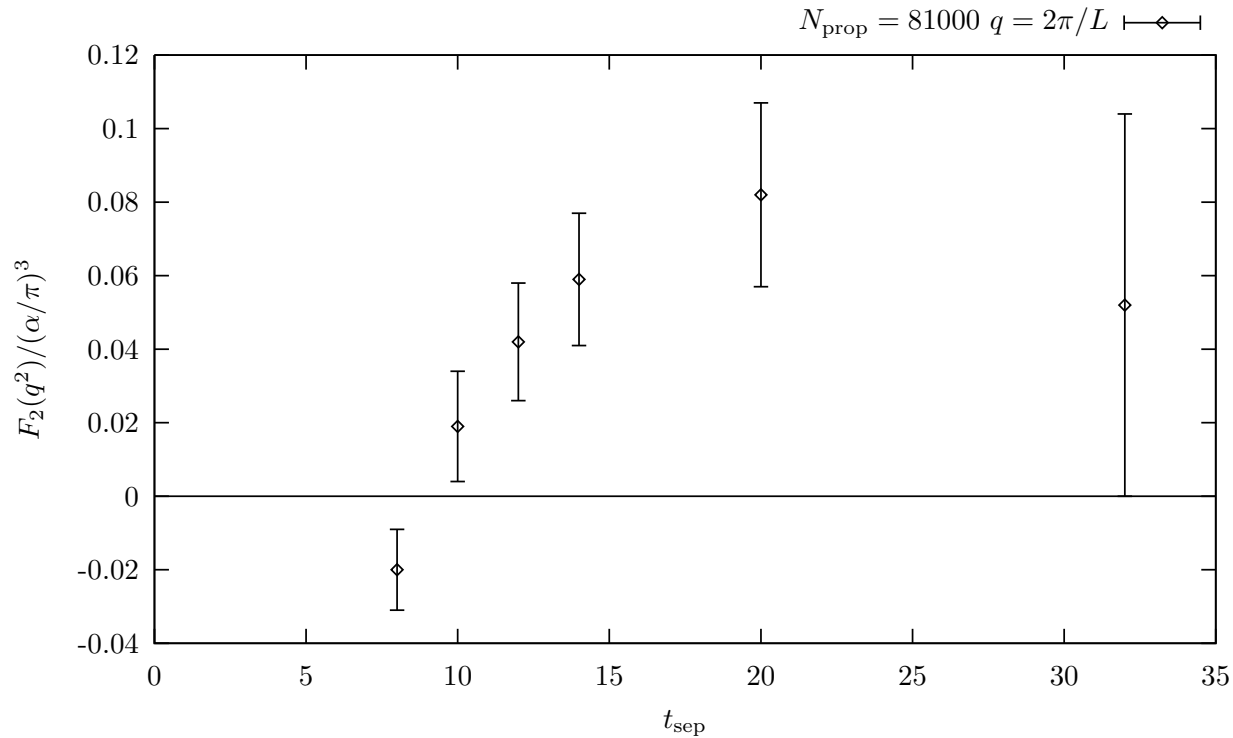
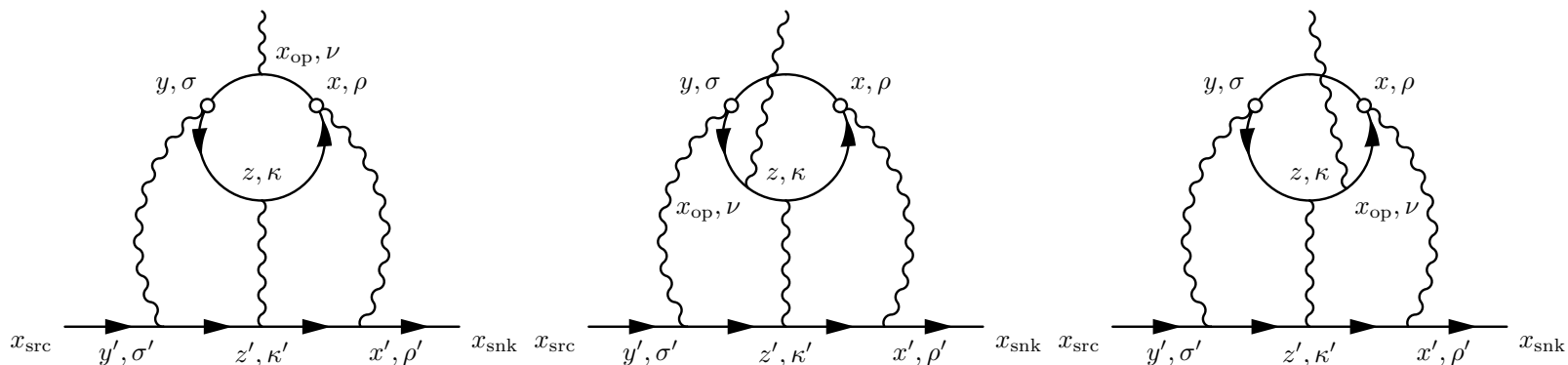
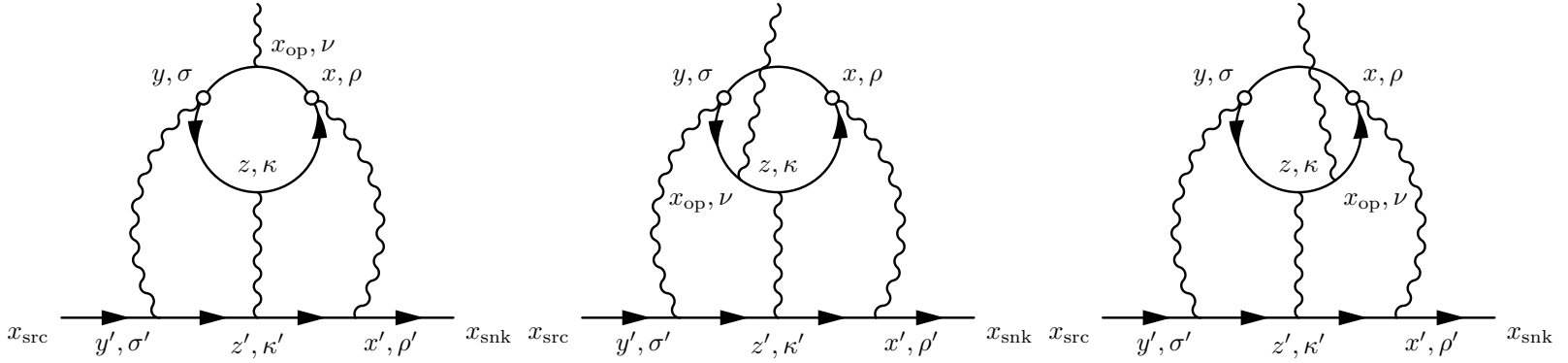


Figure 8. Phys.Rev.Lett. 114 (2015) 1, 012001. arXiv:1407.2923.

- $24^3 \times 64$ lattice with $a^{-1} = 1.747 \text{ GeV}$ and $m_\pi = 333 \text{ MeV}$. $m_\mu = 175 \text{ MeV}$.
- For comparison, at physical point, model estimation is 0.08 ± 0.02 . The agreement is accidental, because the result has a strong dependence on m_μ .



- We can use two point source photons at x and y , which are chosen randomly. It is a very standard 8-dimensional Monte Carlo integral over two space-time points.
- Only the relative coordinate between x and y is relevant. The integration is actually 4-dimensional.
- Major contribution comes from the region where x and y are not far separated. Importance sampling is needed. In fact, we can evaluate all possible (upto discrete symmetries) relative positions for distance less than a certain value r_{\max} , which is normally set to be 5 lattice units. Only 102 pairs are needed to reach r_{\max} .



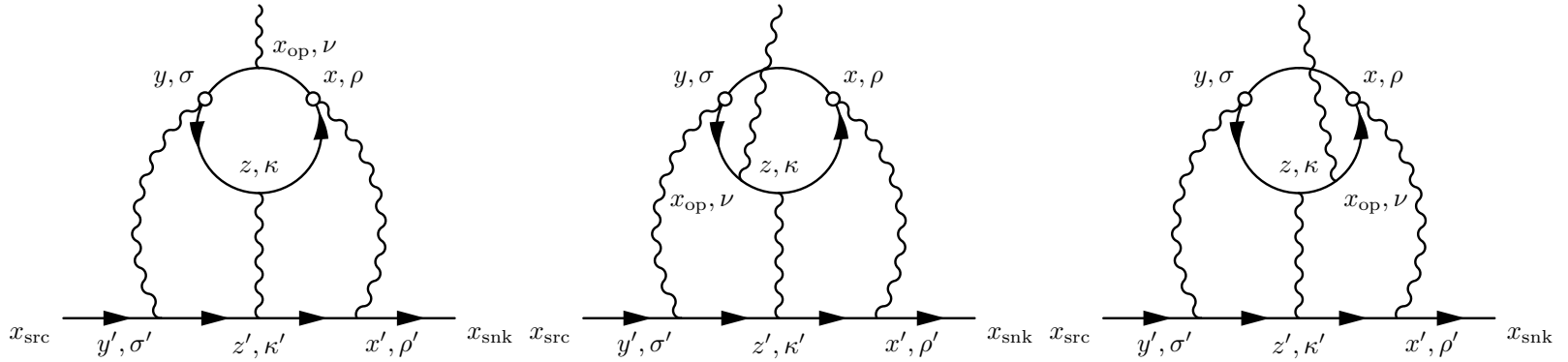
$$\mathcal{M}_{\nu}^{\text{LbL}}(\vec{q}) = \exp(i \vec{q} \cdot \vec{x}_{\text{op}}) \mathcal{M}_{\nu}^{\text{LbL}}(\vec{q}; x_{\text{op}}) \quad (46)$$

$$= \sum_{x, y, z} \exp(i \vec{q} \cdot \vec{x}_{\text{op}}) \mathcal{F}_{\nu}^C(\vec{q}; x, y, z, x_{\text{op}}) \quad (47)$$

with translational invariance $= \sum_r \left[\sum_{z, x_{\text{op}}} \exp(i \vec{q} \cdot \vec{x}_{\text{op}}) \mathcal{F}_{\nu}^C\left(\vec{q}; -\frac{r}{2}, +\frac{r}{2}, z, x_{\text{op}}\right) \right] \quad (48)$

in the small q limit $\approx \sum_r \left[\sum_{z, x_{\text{op}}} (1 + i \vec{q} \cdot \vec{x}_{\text{op}}) \mathcal{F}_{\nu}^C\left(\vec{q}; -\frac{r}{2}, +\frac{r}{2}, z, x_{\text{op}}\right) \right] \quad (49)$

$$= \sum_r \left[\sum_{z, x_{\text{op}}} i \vec{q} \cdot \vec{x}_{\text{op}} \mathcal{F}_{\nu}^C\left(\vec{q}; -\frac{r}{2}, +\frac{r}{2}, z, x_{\text{op}}\right) \right] + \sum_r \sum_{z, x_{\text{op}}} \mathcal{F}_{\nu}^C\left(\vec{q}; -\frac{r}{2}, +\frac{r}{2}, z, x_{\text{op}}\right) \quad (50)$$



$$\mathcal{M}_\nu^{\text{LbL}}(\vec{q}) = \sum_r \left[\sum_{z, x_{\text{op}}} i \vec{q} \cdot \vec{x}_{\text{op}} \mathcal{F}_\nu^C \left(\vec{q}; -\frac{r}{2}, +\frac{r}{2}, z, x_{\text{op}} \right) \right] \quad (51)$$

$$\bar{u}_{s'}(\vec{q}/2) \mathcal{M}_\nu^{\text{LbL}}(\vec{q}) u_s(-\vec{q}/2) = \bar{u}_{s'}(\vec{q}/2) \left(i \frac{F_2(q^2)}{4m} [\gamma_\nu, \gamma_\rho] q_\rho \right) u_s(-\vec{q}/2) \quad (52)$$

Taking $q \rightarrow 0$ limit by computing derivative with respect to q , we obtained the familiar magnetic moment formula.

$$\frac{F_2(0)}{m} \bar{u}_{s'}(\vec{0}) \frac{\vec{\Sigma}}{2} u_s(\vec{0}) = \sum_r \left[\sum_{z, x_{\text{op}}} \frac{1}{2} \vec{x}_{\text{op}} \times \bar{u}_{s'}(\vec{0}) i \vec{\mathcal{F}}^C \left(\vec{0}; -\frac{r}{2}, +\frac{r}{2}, z, x_{\text{op}} \right) u_s(\vec{0}) \right] \quad (53)$$

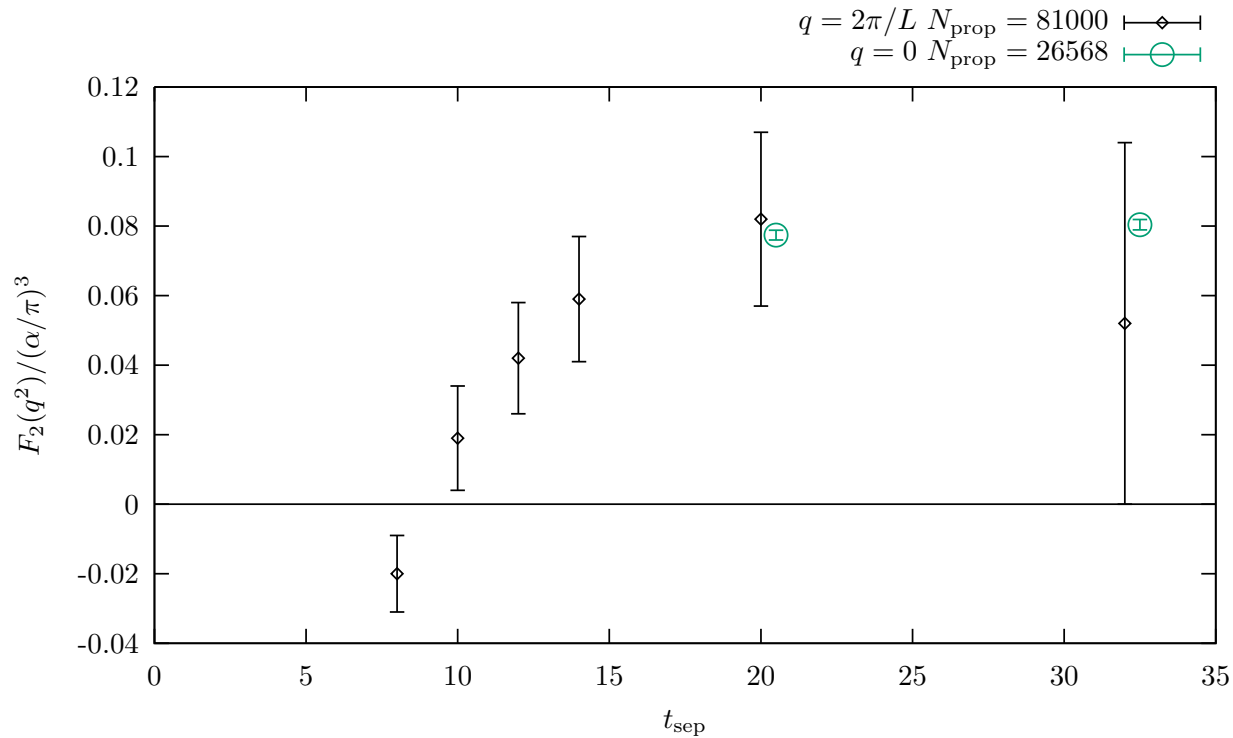
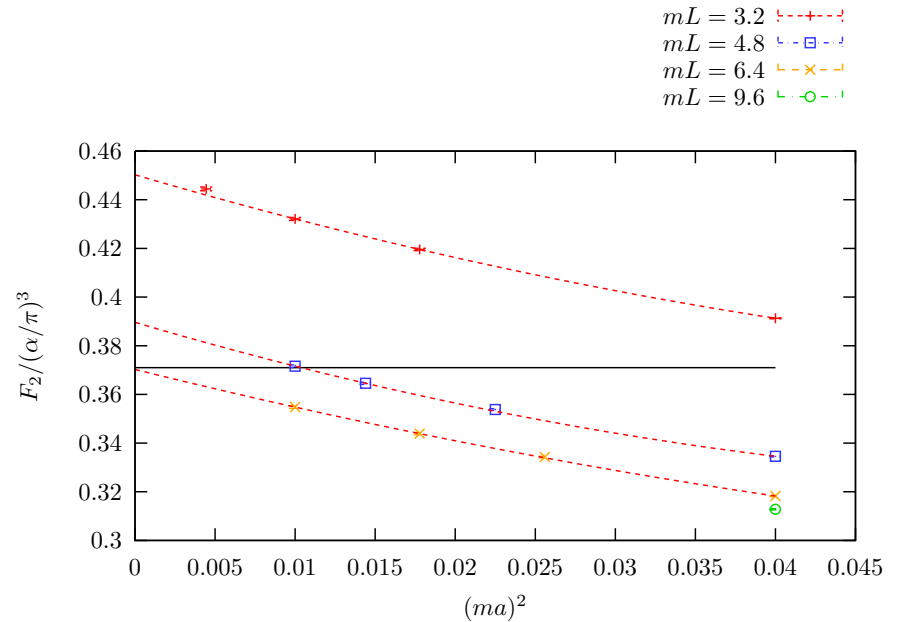
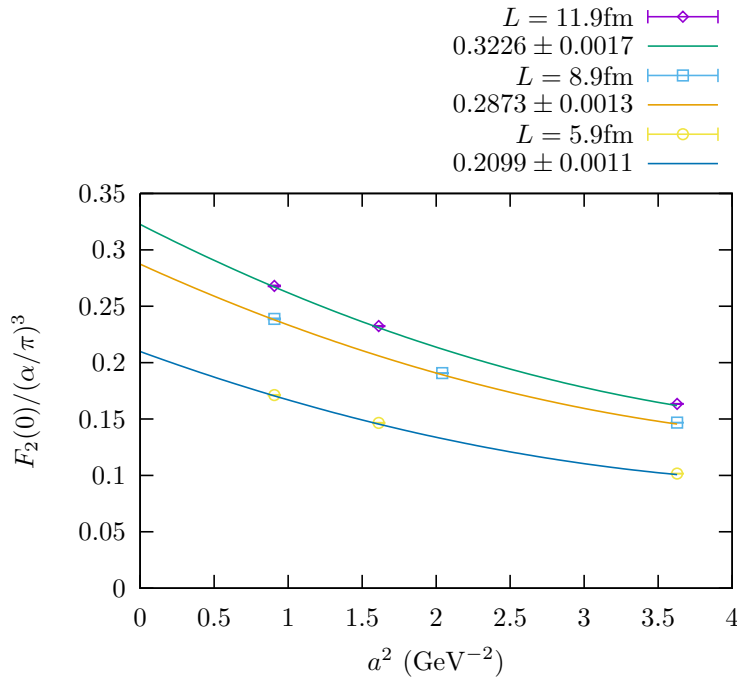


Figure 9. Phys.Rev.Lett. 114 (2015) 1, 012001. Compare with the latest method and result.

- $24^3 \times 64$ lattice with $a^{-1} = 1.747 \text{ GeV}$ and $m_\pi = 333 \text{ MeV}$. $m_\mu = 175 \text{ MeV}$.
- For comparison, at physical point, model estimation is 0.08 ± 0.02 . The agreement is accidental, because the result has a strong dependence on m_μ .

- We test our setup by computing **muon leptonic light by light** contribution to muon $g - 2$.



- Pure QED computation.** Muon leptonic light by light contribution to muon $g - 2$.
- Left: $\mathcal{O}(1/L^2)$ finite volume effect, because the photons are emitted from a conserved loop. Phys.Rev. D93 (2016) 1, 014503.
- Right: $\mathcal{O}(e^{-mL})$ finite volume effect. Everything except the four-point-correlation function is evaluated in infinite volume.



For the four-point-function, when its two ends, x and y , are far separated, but x' is close to x and y' is close to y , the four-point-function is dominated by π^0 exchange.

Both the connected and the disconnected diagram will contribute in these region. We can find a connection between the connected diagram and the disconnected diagram by first investigating the η correlation function.

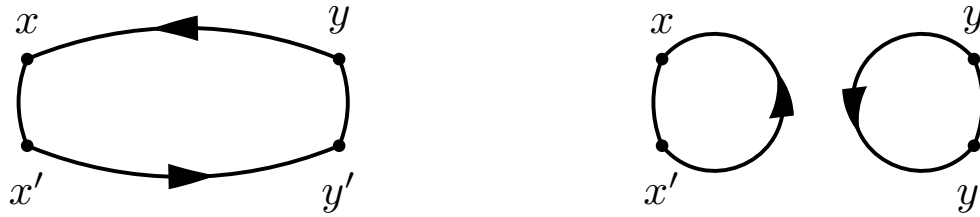
$$\langle \bar{u}\gamma_5 u(x)(\bar{u}\gamma_5 u + \bar{d}\gamma_5 d)(y) \rangle \sim e^{-m_\eta|x-y|} \quad (54)$$

$$\langle \bar{u}\gamma_5 u(x)(\bar{u}\gamma_5 u - \bar{d}\gamma_5 d)(y) \rangle + 2\langle \bar{u}\gamma_5 u(x)\bar{d}\gamma_5 d(y) \rangle \sim e^{-m_\eta|x-y|} \quad (55)$$

That is

$$\langle \bar{u}\gamma_5 u(x)\bar{d}\gamma_5 d(y) \rangle = -\frac{1}{2}\langle \bar{u}\gamma_5 u(x)(\bar{u}\gamma_5 u - \bar{d}\gamma_5 d)(y) \rangle + \mathcal{O}(e^{-m_\eta|x-y|}) \quad (56)$$

Above is a relation between disconnected diagram π^0 exchange (left hand side) and connected diagram π^0 exchange (right hand side).



The nearby two current operator can be viewed as an interpolating operator for π^0 , just like $\bar{u}\gamma_5 u$ or $\bar{d}\gamma_5 d$ with appropriate charge factors.

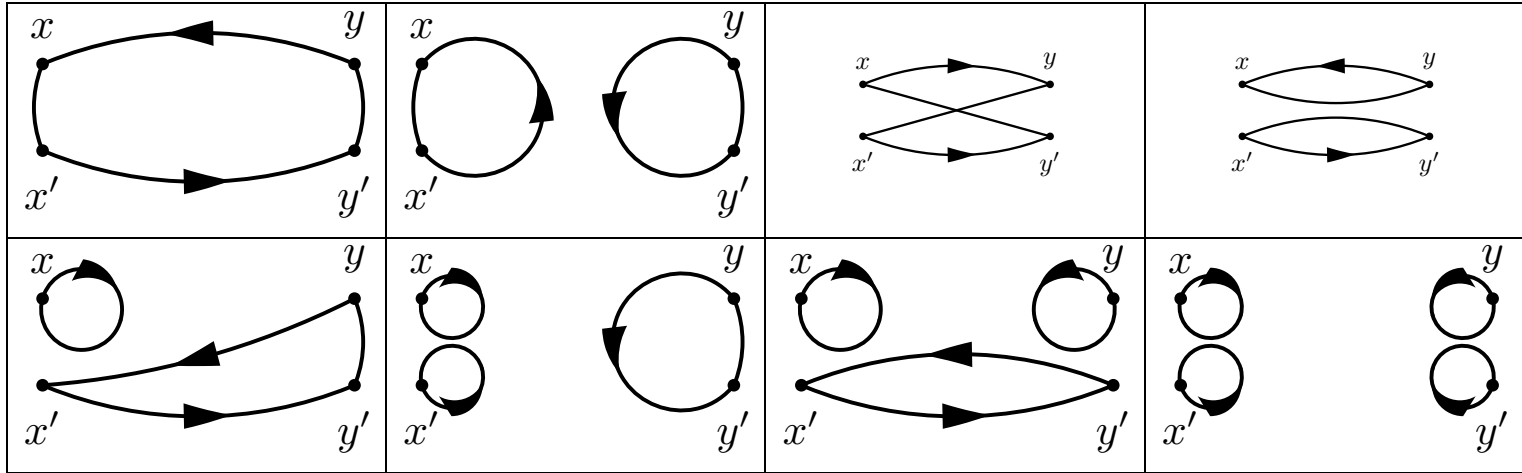
Multiplied by appropriate charge factors:

$$\text{Connected contribution} \quad \left[\left(\frac{2}{3} \right)^4 + \left(-\frac{1}{3} \right)^4 \right] = \frac{17}{81} \quad (57)$$

$$\text{Disconnected contribution} \quad \left[\left(\frac{2}{3} \right)^2 + \left(-\frac{1}{3} \right)^2 \right]^2 \left(-\frac{1}{2} \right) = \frac{25}{81} \left(-\frac{1}{2} \right) \quad (58)$$

$$\text{Connected : Disconnected} = 34 : -25 \quad (59)$$

Different approach by J. Bijnens and J. Relefors: **JHEP 1609 (2016) 113**.



$$J_\mu(x) = e_u \bar{u} \gamma_\mu u(x) + e_d \bar{d} \gamma_\mu d(x) \quad ; \quad V_\mu(x) = \bar{u} \gamma_\mu u(x) - \bar{d} \gamma_\mu d(x) \quad (60)$$

$$\langle J_\mu(x) J_\nu(x') J_\rho(y) J_\sigma(y') \rangle \sim e^{-m_\pi |x-y|} \quad (61)$$

$$\langle V_\mu(x) V_\nu(x') V_\rho(y) V_\sigma(y') \rangle \sim e^{-2m_\pi |x-y|} \quad (62)$$

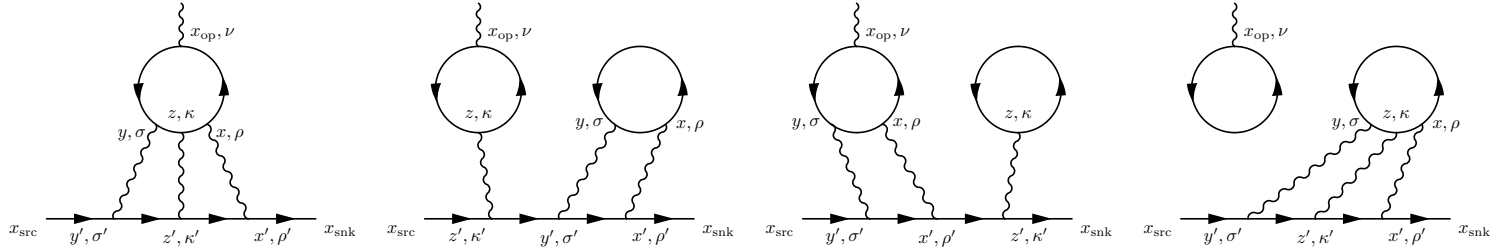
The four-point function $\langle V_\mu(x) V_\nu(x') V_\rho(y) V_\sigma(y') \rangle$ is

- Very small in large separation limit.
- Only composed diagrams in the first row.

The contribution from the first two diagrams must cancel among themselves. Leads to ratio obtained in previous slides. 34: -25 (first two, first row)

Similarly, we can obtain: 14: -5 (first two, second row), 10: -1 (last two, second row).

When the 4 points of the 4-point function are all far separated:



$(e_u^4 + e_d^4)C$ Connected diagram contribution

$(e_u^2 + e_d^2)^2 D$ Leading order disconnected diagram contribution

$(e_u + e_d)(e_u^3 + e_d^3) D'$ Next leading order disconnected diagram contribution

$$\begin{aligned} \mathcal{M} &\approx (e_u^4 + e_d^4) C + (e_u^2 + e_d^2)^2 D + (e_u + e_d)(e_u^3 + e_d^3) D' \\ &\propto (e_u - e_d)^4 \end{aligned} \quad (63)$$

$$C : D : D' = -2 : -3 : 4 \quad (64)$$

$$\text{Connected} : \text{LO-disconnected} : \text{NLO-disconnected} = -34 : -75 : 28 \quad (65)$$

Study the spatial component,

$$\langle \mathbf{p}', s' | i \mathbf{j}(\mathbf{x}_{\text{op}} = 0) | \mathbf{p}, s \rangle = -e \bar{u}_{s'}(\mathbf{p}') \left[F_1(q^2) i \boldsymbol{\gamma} - \frac{F_2(q^2)}{m} i \mathbf{q} \times \frac{\boldsymbol{\Sigma}}{2} \right] u_s(\mathbf{p}) \quad (66)$$

$$[\gamma_i, \gamma_j] = 2 i \epsilon_{ijk} \Sigma_k \quad (67)$$

With Gordon identity

$$\bar{u}_{s'}(\mathbf{p}') i \boldsymbol{\gamma} u_s(\mathbf{p}) = \bar{u}_{s'}(\mathbf{p}') \left(\frac{\mathbf{p}' + \mathbf{p}}{2m} - \frac{1}{m} i \mathbf{q} \times \frac{\boldsymbol{\Sigma}}{2} \right) u_s(\mathbf{p}) \quad (68)$$

$$\begin{aligned} & \langle \mathbf{p}', s' | i \mathbf{j}(\mathbf{x}_{\text{op}} = 0) | \mathbf{p}, s \rangle \\ = & -e \bar{u}_{s'}(\mathbf{p}') \left[F_1(q^2) \frac{\mathbf{p}' + \mathbf{p}}{2m} - \frac{F_1(q^2) + F_2(q^2)}{m} i \mathbf{q} \times \frac{\boldsymbol{\Sigma}}{2} \right] u_s(\mathbf{p}) \end{aligned} \quad (69)$$

Consider a normalized state

$$|\psi\rangle = \int \frac{d^3p}{(2\pi)^3} |\mathbf{p}, s\rangle \psi_s(\mathbf{p}) \quad (70)$$

We require the state with the momentum almost zero and the expectation value of the current exactly zero:

$$\int d^3x_{\text{op}} \langle \psi | i \mathbf{j}(\mathbf{x}_{\text{op}}) | \psi \rangle = 0 \quad (71)$$

We then consider the following amplitude with extremely small $\mathbf{q} \ll \Delta\mathbf{p} \sim 1/\Delta\mathbf{x}$.

$$\mathcal{M} = \int d^3x_{\text{op}} \exp(i \mathbf{q} \cdot \mathbf{x}_{\text{op}}) \langle \psi | i \mathbf{j}(\mathbf{x}_{\text{op}}) | \psi \rangle \quad (72)$$

We can safely subtract zero

$$\begin{aligned} \mathcal{M} &= \int d^3x_{\text{op}} [\exp(i \mathbf{q} \cdot \mathbf{x}_{\text{op}}) - 1] \langle \psi | i \mathbf{j}(\mathbf{x}_{\text{op}}) | \psi \rangle \\ &\approx \int d^3x_{\text{op}} i \mathbf{q} \cdot \mathbf{x}_{\text{op}} \langle \psi | i \mathbf{j}(\mathbf{x}_{\text{op}}) | \psi \rangle \end{aligned} \quad (73)$$

On the other hand, with momentum conservation

$$\begin{aligned} \mathcal{M} = & -e \int \frac{d^3 p}{(2\pi)^3} \psi_{s'}^*(\mathbf{p} + \mathbf{q}/2) \psi_s(\mathbf{p} - \mathbf{q}/2) \\ & \cdot \bar{u}_{s'}(\mathbf{p} + \mathbf{q}/2) \left[F_1(q^2) \frac{\mathbf{p}}{m} - \frac{F_1(q^2) + F_2(q^2)}{m} i \mathbf{q} \times \frac{\boldsymbol{\Sigma}}{2} \right] u_s(\mathbf{p} - \mathbf{q}/2) \end{aligned} \quad (74)$$

The second term is explicitly $\mathcal{O}(\mathbf{q})$, the first term must be at most $\mathcal{O}(\mathbf{q})$ as well. The magnetic moment of a fermion could result from its orbital angular momentum even if its momentum is small, because of large size. One way we can eliminate that is to require $\psi_s^*(\mathbf{p}) = \psi_s(\mathbf{p})$, so that the $\mathcal{O}(\mathbf{q})$ part of the first term vanishes. Only keep the leading $\mathcal{O}(\mathbf{q})$ term, we obtain

$$\mathcal{M} \approx e \frac{F_1(q^2=0) + F_2(q^2=0)}{m} i \mathbf{q} \times \left\langle \frac{\boldsymbol{\Sigma}}{2} \right\rangle \quad (75)$$

$$\left\langle \frac{\boldsymbol{\Sigma}}{2} \right\rangle = \int \frac{d^3 p}{(2\pi)^3} \psi_{s'}^*(\mathbf{p}) \psi_s(\mathbf{p}) \bar{u}_{s'}(\mathbf{p}) \frac{\boldsymbol{\Sigma}}{2} u_s(\mathbf{p}) \quad (76)$$

Combine the results from previous two approaches:

$$e \frac{F_1(q^2=0) + F_2(q^2=0)}{m} i \mathbf{q} \times \left\langle \frac{\mathbf{\Sigma}}{2} \right\rangle \approx \int d^3 x_{\text{op}} i \mathbf{q} \cdot \mathbf{x}_{\text{op}} \langle \psi | i \mathbf{j}(\mathbf{x}_{\text{op}}) | \psi \rangle \quad (77)$$

Cancel the \mathbf{q} , we obtain

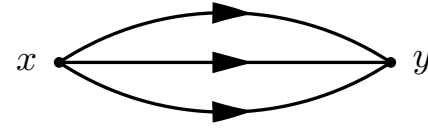
$$e \frac{F_1(q^2=0) + F_2(q^2=0)}{m} \epsilon_{ijk} \left\langle \frac{\Sigma_k}{2} \right\rangle = \int d^3 x_{\text{op}} (x_{\text{op}})_j \langle \psi | i j_i(\mathbf{x}_{\text{op}}) | \psi \rangle \quad (78)$$

Finally

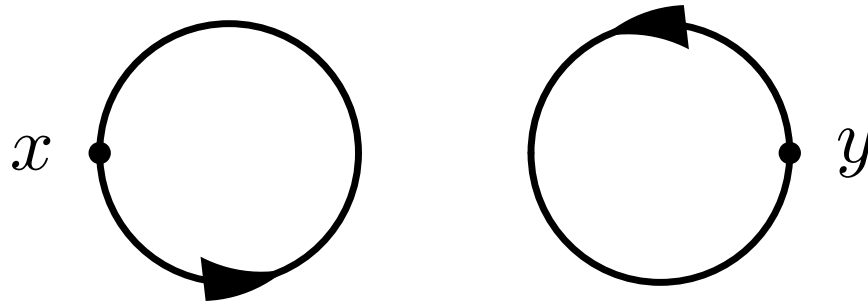
$$-e \frac{F_1(q^2=0) + F_2(q^2=0)}{m} \left\langle \frac{\mathbf{\Sigma}}{2} \right\rangle = \left\langle \psi \left| \int \frac{1}{2} \mathbf{x}_{\text{op}} \times i \mathbf{j}(\mathbf{x}_{\text{op}}) d^3 x_{\text{op}} \right| \psi \right\rangle \quad (79)$$

- e.g. Pion correlation function with non-zero momentum: Noise $\sim e^{-m_\pi|y-x|}$.

- e.g. Proton correlation function: Noise $\sim e^{-\frac{3m_\pi}{2}|y-x|}$.



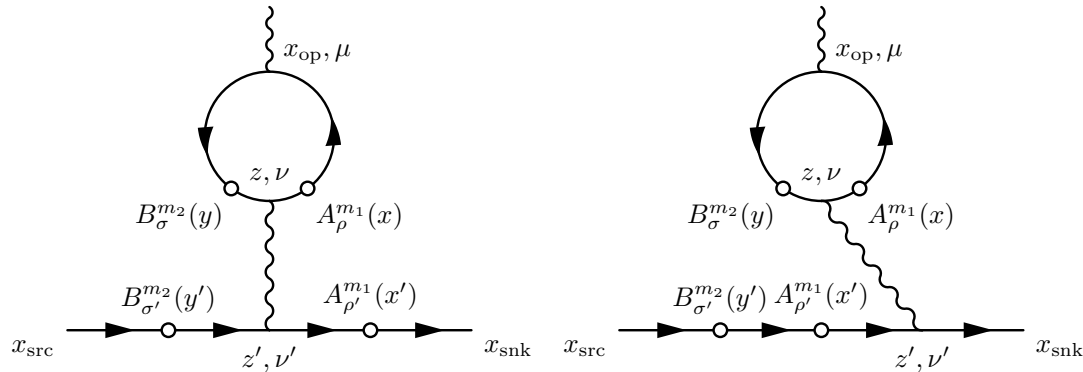
There is one kind of correlation without the fermion line connected to both ends. This kind of diagrams is called the “disconnected diagram”. The size of the noise is roughly independent of separation. For example:



$$\langle \bar{d}(y) \gamma_5 d(y) \bar{u}(x) \gamma_5 u(x) \rangle_{\text{QCD}} = \langle \text{Tr}[\gamma_5 S_l(y, y)] \text{Tr}[\gamma_5 S_l(x, x)] \rangle_{\text{QCD}} \quad (80)$$

$$\sim \frac{e^{-m_\pi|y-x|}}{|y-x|^{3/2}} \sim e^{-m_\pi|y-x|} \quad (81)$$

- Only evaluate the $\mathcal{O}(e^6)$ term. No lower order noise, no contribution from higher order diagrams.



PoS(LATTICE2014)130. Light by Light diagrams calculated with one exact photon and two stochastic photon. There are 4 other possible permutations.

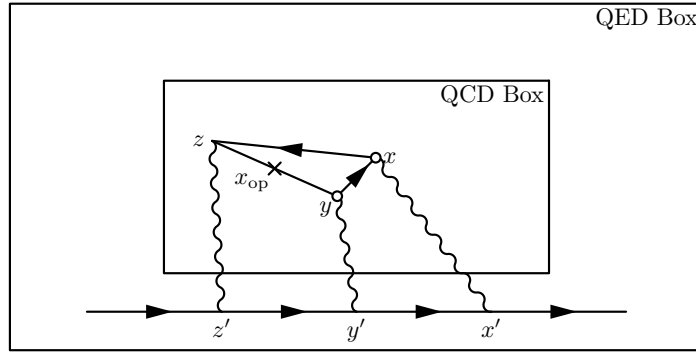
$$G_{\mu\nu}(x, y) \approx \frac{1}{M} \sum_{m=1}^M A_{\nu}^m(x) A_{\nu'}^m(y) \quad (82)$$

- Diagram can be evaluated with sequential source propagators and independent QED gauge fields.
- “Disconnect diagram” problem is still there. Noise will increase in larger volume.

$$\begin{aligned}
& \frac{F_2^{\text{cHLbL}}(q^2=0)}{m} \frac{(\sigma_{s',s})_i}{2} \\
&= \sum_{r, \tilde{z}} \Im \left(\frac{r}{2}, -\frac{r}{2}, \tilde{z} \right) \sum_{\tilde{x}_{\text{op}}} \frac{1}{2} \epsilon_{i,j,k} (\tilde{x}_{\text{op}})_j \cdot i \bar{u}_{s'}(\vec{0}) \mathcal{F}_k^C \left(\frac{r}{2}, -\frac{r}{2}, \tilde{z}, \tilde{x}_{\text{op}} \right) u_s(\vec{0}) \quad (83)
\end{aligned}$$

$$\begin{aligned}
& \mathcal{F}_\nu^C(x, y, z, x_{\text{op}}) = (-ie)^6 \mathcal{G}_{\rho, \sigma, \kappa}(x, y, z) \sum_{q=u,d,s} (e_q/e)^4 \quad (84) \\
& \times \frac{1}{3} \left\langle \text{tr} \left[-\gamma_\rho S_q(x, z) \gamma_\kappa S_q(z, y) \gamma_\sigma S_q(y, x_{\text{op}}) \gamma_\nu S_q(x_{\text{op}}, x) \right] + \text{other 2 permutations} \right\rangle_{\text{QCD}}
\end{aligned}$$

- The integrand decreases exponentially if one of r , z , or x_{op} become large. The fact that the sum is limited within the lattice only has exponentially suppressed effect. We have use the moment method to take $q \rightarrow 0$ limit, eliminating that part of the “finite volume” effect.
- However, $\mathcal{G}(x, y, z)$ involves massless photon propagators. Thus, evaluating this function in a small volume leads to $\mathcal{O}(1/L^2)$ finite volume effects.
- Solution: do not evaluate $\mathcal{G}(x, y, z)$ within the QCD box. We evaluate it in larger QED boxes. We are also working on numerical strategies to compute the sum in infinite volume. This way, we can capture the major part of the finite volume effects with the QCD lattice just large enough to contain the quark loop.



$$\mathcal{F}_\nu^C(x, y, z, x_{\text{op}}) = (-ie)^6 \mathcal{G}_{\rho, \sigma, \kappa}(x, y, z) \sum_{q=u, d, s} (e_q/e)^4 \quad (85)$$

$$\times \frac{1}{3} \left\langle \text{tr} \left[-\gamma_\rho S_q(x, z) \gamma_\kappa S_q(z, y) \gamma_\sigma S_q(y, x_{\text{op}}) \gamma_\nu S_q(x_{\text{op}}, x) \right] + \text{other 2 permutations} \right\rangle_{\text{QCD}}$$

$$= \mathcal{G}_{\rho, \sigma, \kappa}(x, y, z) \quad (86)$$

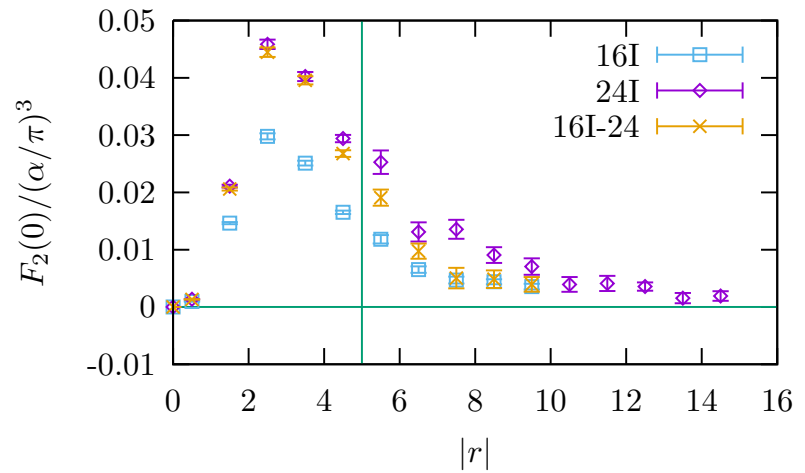
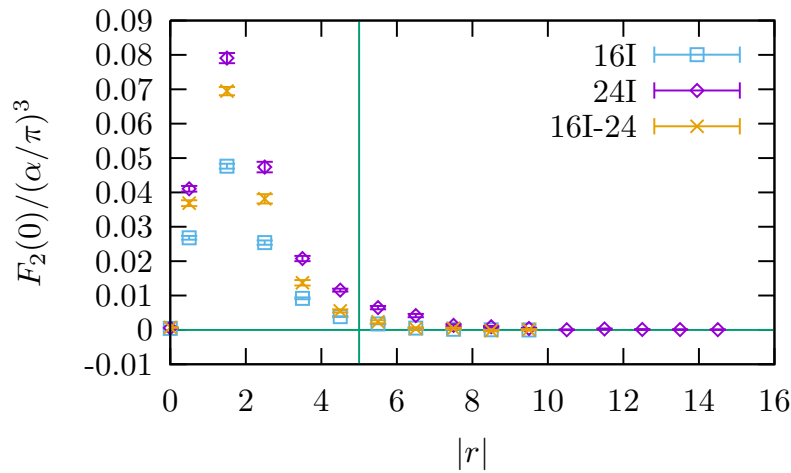
$$= e^{m_\mu(t_{\text{snk}} - t_{\text{src}})} \sum_{x', y', z'} G_{\rho, \rho'}(x, x') G_{\sigma, \sigma'}(y, y') G_{\kappa, \kappa'}(z, z')$$

$$\cdot \sum_{\vec{x}_{\text{snk}}, \vec{x}_{\text{src}}} [S_\mu(x_{\text{snk}}, x') \gamma_{\rho'} S_\mu(x', z') \gamma_{\kappa'} S_\mu(z', y') \gamma_{\sigma'} S_\mu(y', x_{\text{src}}) + S_\mu(x_{\text{snk}}, z') \gamma_{\kappa'} S_\mu(z', x') \gamma_{\rho'} S_\mu(x', y') \gamma_{\sigma'} S_\mu(y', x_{\text{src}}) + \text{other 4 permutations}].$$

Ensemble	$m_\pi L$	QCD Size	QED Size	$\frac{F_2(q^2=0)}{(\alpha/\pi)^3}$
16l	3.87	$16^3 \times 32$	$16^3 \times 32$	0.1158(8)
24l	5.81	$24^3 \times 64$	$24^3 \times 64$	0.2144(27)
16l-24		$16^3 \times 32$	$24^3 \times 64$	0.1674(22)

Table 5. arXiv:1511.05198. Finite volume effects studies. $a^{-1} = 1.747$ GeV, $m_\pi = 423$ MeV, $m_\mu = 332$ MeV.

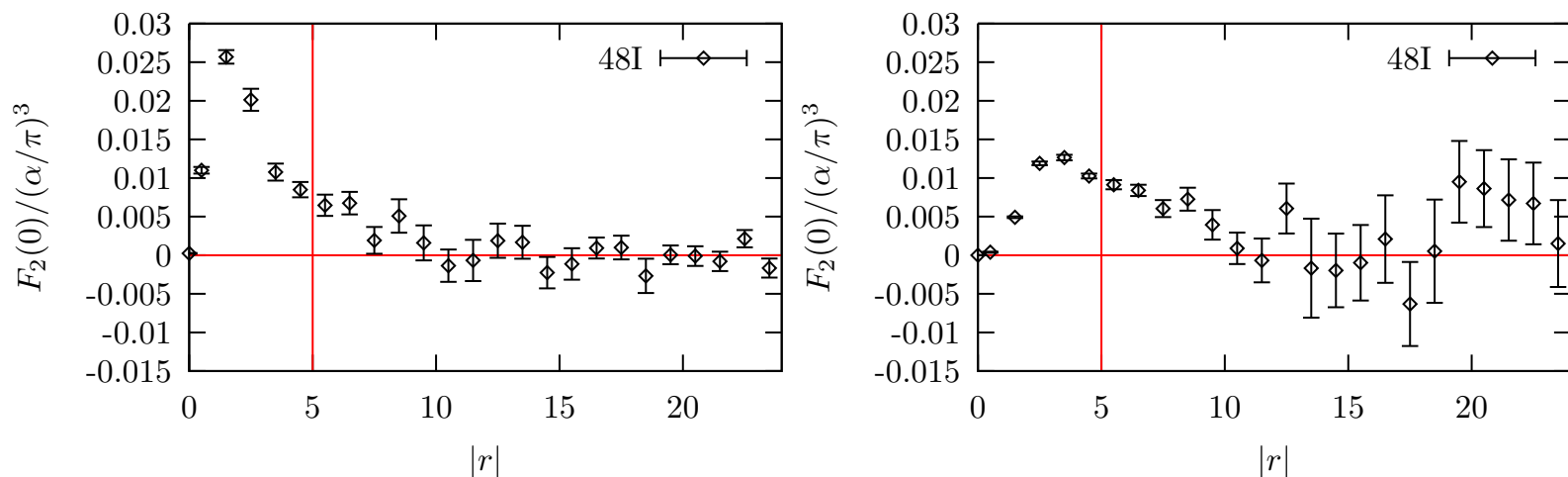
- Large finite volume effects with these ensembles and muon mass.
- Increasing the QED box size help reducing the finite volume effect, but haven't completely fixed the problem.
- Suggesting significant QCD finite volume effect.
- The histogram plot may help us further investigating this QCD finite volume effect.



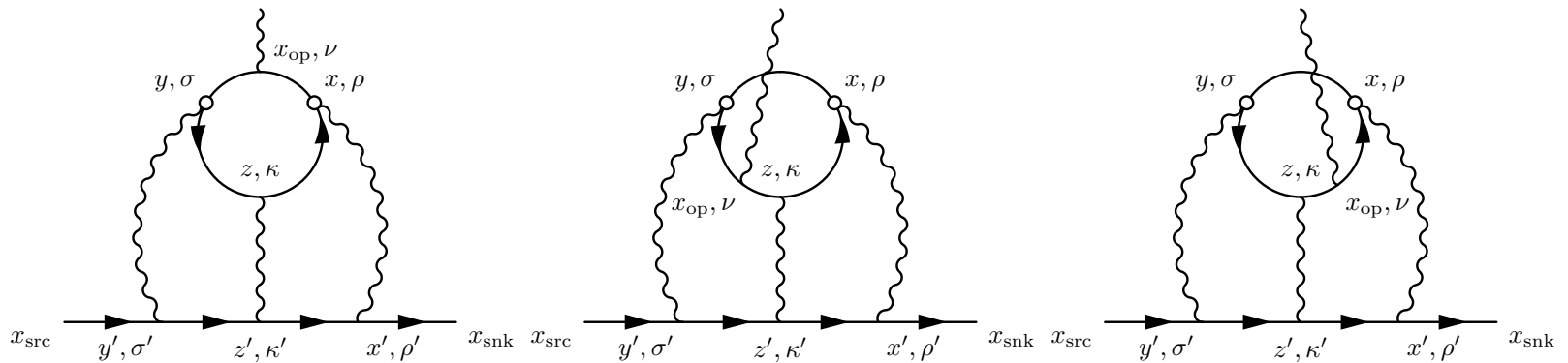
- arXiv:1511.05198. Above plots show histograms of the contribution to F_2 from different separations $|r| = |x - y|$. The sum of all these points gives the final result for F_2 . The vertical lines at $|r| = 5$ in the plots indicate the value of r_{max} .
- The left plot is evaluated with z summed over longer distance region, so the small r region includes most of the contribution.
- The right plot is evaluated with z summed over longer distance region, so the QCD finite volume is better controlled in the small r region.

$$\sum_z \quad \text{v.s.} \quad \sum_z$$

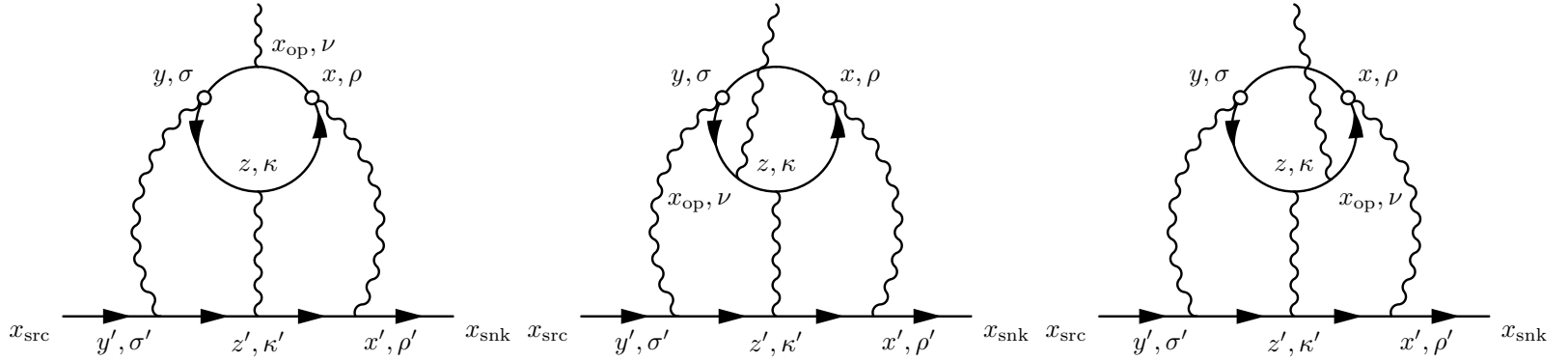
$$|x-y| < \min(|x-z|, |y-z|) \quad |x-y| > \max(|x-z|, |y-z|)$$



- $48^3 \times 96$ lattice, with $a^{-1} = 1.73\text{GeV}$, $m_\pi = 139\text{MeV}$, $m_\mu = 106\text{MeV}$.
- The left plot is evaluated with z summed over longer distance region, so the small r region includes most of the contribution.
- The right plot is evaluated with z summed over shorter distance region, so the QCD finite volume is better controlled in the small r region.
- Contribution vanishes long before reaching the boundary of the lattice.
- Suggesting the QCD finite volume effects be small in this case.
- Simply increasing the QED box will fix most of the finite volume effects.



- The points x , y , z are equivalent, we are free to re-label them.
- Since we sum over z , but sample over $r = y - x$. It is beneficial to keep r small, where the fluctuation is small and sampling can be complete.
- So, when we sum over z , we only sum the region where z is far from x , y compare with the distance between x and y .
- This way, we **move** most of the contribution into the small r region, where the fluctuation is small and sampling can be complete.



$$\begin{aligned}
 & \frac{F_2^{\text{cHLbL}}(0)}{m} \frac{(\sigma_{s',s})_i}{2} \\
 &= \sum_{r, \tilde{z}} \mathfrak{Z}\left(\frac{r}{2}, -\frac{r}{2}, \tilde{z}\right) \sum_{\tilde{x}_{\text{op}}} \frac{1}{2} \epsilon_{i,j,k}(\tilde{x}_{\text{op}})_j \cdot i \bar{u}_{s'}(\vec{0}) \mathcal{F}_k^C\left(\frac{r}{2}, -\frac{r}{2}, \tilde{z}, \tilde{x}_{\text{op}}\right) u_s(\vec{0}) \quad (87)
 \end{aligned}$$

$$\mathfrak{Z}(x, y, z) = \begin{cases} 3 & \text{if } |x - y| < |x - z| \text{ and } |x - y| < |y - z| \\ 3/2 & \text{if } |x - y| = |x - z| < |y - z| \text{ or } |x - y| = |y - z| < |x - z| \\ 1 & \text{if } |x - y| = |x - z| = |y - z| \\ 0 & \text{otherwise} \end{cases} \quad (88)$$